YANKEE ATOMIC ELECTRIC COMPANY

YAEC-1844

Vermont Yankee
Cycle 16
Core Performance Analysis Report

YANKEE

Prepared by: M A Sironen — 2/7/92
M. A. Sironen — (Date)
Nuclear Engineering Coordinator

Approved by: R J Cacciapouti — 2/10/92
R. J. Cacciapouti, Manager — (Date)
Reactor Physics Group

Approved by: P.A. Bergeron — 2/10/92
P. A. Bergeron, Manager — (Date)
Transient Analysis Group

Approved by: R Sundaram — 2/10/92
R. K. Sundaram, Manager — (Date)
LOCA Analysis Group

Approved by: B C Slifer — 2/10/92
B. C. Slifer, Director — (Date)
Nuclear Engineering Department

Yankee Atomic Electric Company
Nuclear Services Division
580 Main Street
Bolton, Massachusetts 01740

DISCLAIMER OF RESPONSIBILITY

This document was prepared by Yankee Atomic Electric Company ("Yankee"). The use of information contained in this document by anyone other than Yankee, or the Organization for which this document was prepared under contract, is not authorized and, with respect to any unauthorized use, neither Yankee nor its officers, directors, agents, or employees assume any obligation, responsibility, or liability or make any warranty or representation as to the accuracy or completeness of the material contained in this document.

ABSTRACT

This report presents design information, calculational results, and operating limits pertinent to the operation of Cycle 16 of the Vermont Yankee Nuclear Power Station. These include the fuel design and core loading pattern descriptions; calculated reactor power distributions, exposure distributions, shutdown capability, and reactivity data; and the results of safety analyses performed to justify plant operation throughout the cycle.

TABLE OF CONTENTS

WPP40/10

TABLE OF CONTENTS
(Continued)

LIST OF FIGURES

<u>LIST OF FIGURES</u>
(Continued)

WPP40/10

LIST OF TABLES

ACKNOWLEDGEMENTS

The author and major contributors would like to acknowledge the contributions to this work by the YAEC Word Processing Center. Their assistance in preparing this document is recognized and greatly appreciated.

1.0 INTRODUCTION

This report provides information to support the operation of the Vermont Yankee Nuclear Power Station through the forthcoming Cycle 16. In this report, Cycle 16 will frequently be referred to as the Reload Cycle. The preceding Cycle 15 will frequently be referred to as the Current Cycle. The refueling between the two will involve the discharge of 128 irradiated fuel bundles and the insertion of 128 new fuel bundles. The resultant core will consist of 128 new fuel bundles and 240 irradiated fuel bundles. The General Electric Company (GE) manufactured all the bundles, except four qualification fuel bundles manufactured by Siemens Nuclear Power (SNP), formerly known as Advanced Nuclear Fuels (ANF). Some of the irradiated fuel was also present in the reactor in Cycle 14. This cycle will frequently be referred to as the Past Cycle.

This report contains descriptions and analyses results pertaining to the mechanical, thermal-hydraulic, physics, and safety aspects of the Reload Cycle. The analyses assumed the reload core contained all GE bundles. This is justified because the SNP bundles were designed to match the GE bundles Section 9.0 describes the Reload Cycle Core Component Qualification Program and its impact on the analyses. The MAPLHGR and MCPR operating limits calculated for the Reload Cycle are given in Appendix A. These limits will be included in the Core Operating Limits Report.

2.0 RECENT REACTOR OPERATING HISTORY

2.1 Operating History of the Current Cycle

The current operating cycle is Cycle 15. To date, the Current Cycle has been operating at, or near, full power with the exception of sequence exchanges, a one short repair outage, four scrams, and a ccastdown to the end of cycle. The operating history highlights and control rod sequence exchange schedule of the Current Cycle are found in Table 2.1.1.

2.2 Operating History of Past Applicable Cycle

The irradiated fuel in the Reload Cycle includes some fuel bundles initially inserted in Cycle 14. This Past Cycle operated at, or near, full power with the exception of sequence exchanges, a short repair outage, two scrams and a coastdown to the end of cycle. The operating history highlights of the Past Cycle are found in Table 2.2.1. The Past Cycle is described in detail in the Cycle 14 Summary Report[1].

TABLE 2.1.1

VY Cycle 15 Operating Highlights

Beginning of Cycle Date	October 14, 1990
End of Cycle Date	March 7, 1992*
Weight of Uranium As-Loaded (Short Tons)	72.95
Beginning of Cycle Core Average Exposure** (MWd/St)	10809
End of Full Power Core Average Exposure** (MWd/St)	20069
End of Cycle Core Average Exposure** (MWd/St)	20930*
Number of Fresh Assemblies	128
Number of Irradiated Assemblies	240

Control Rod Sequence Exchange Schedule:

Date	Sequence From	To
December 15, 1990	A2-1	B1-1
January 28, 1991	B1-1	B2-1
March 12, 1991	B2-1	A1-1
May 19, 1991	A1-1	A2-2
July 21, 1991	A2-2	B1-2
September 14, 1991	B1-2	B2-2
November 23, 1991	B2-2	A1-2

* Projected dates and exposures.

** According to the Plant Process Computer.

TABLE 2.2.1

VY Cycle 14 Operating Highlights

Beginning of Cycle Date	April 8, 1989
End of Cycle Date	August 31, 1990
Weight of Uranium As-Loaded (Short Tons)	73.94
Beginning of Cycle Core Average Exposure* (MWd/St)	9195
End of Full Power Core Average Exposure* (MWd/St)	18343
End of Cycle Core Average Exposure* (MWd/St)	19642
Number of Fresh Assemblies	136
Number of Irradiated Assemblies	232

Control Rod Sequence Exchange Schedule:

Date	Sequence From	Sequence To
June 3, 1989	A2-1	B1-1
July 29, 1989	B1-1	A1-1
September 23, 1989	A1-1	B2-1
November 18, 1989	B2-1	A2-2
January 6, 1990	A2-2	B1-2
March 21, 1990	B1-2	A1-2
May 19, 1990	A1-2	B2-2
July 7, 1990	B2-2	A2-3

* According to the Plant Process Computer.

3.0 RELOAD CORE DESIGN DESCRIPTION

3.1 Core Fuel Loading

The Reload Cycle core will consist of both new and irradiated assemblies. All the assemblies have bypass flow holes drilled in the lower tie plate. Table 3.1.1 characterizes the core by fuel type, batch size, and first cycle loaded. A description of the fuel is found in the GE Standard Application for Reactor Fuel[2].

3.2 Design Reference Core Loading Pattern

The Reload Cycle assembly locations are indicated on the map in Figure 3.2.1. For the sake of legibility only the lower right quadrant is shown. The other quadrants are mirror images with bundles of the same type having nearly identical exposures. The bundles are identified by the reload number in which they were first introduced into the core. If any changes are made to the loading pattern at the time of refueling, they will be evaluated under 10CFR50.59. The final loading pattern with specific bundle serial numbers will be supplied in the Startup Test Report.

3.3 Assembly Exposure Distribution

The assumed nominal exposure on the fuel bundles in the Reload Cycle design reference loading pattern is given in Figure 3.2.1. To obtain this exposure distribution, the Past Cycle was depleted with the SIMULATE-3 model[3],[4] using actual plant operating history. For the Current Cycle, plant operating history was used through March 28, 1991. Beyond this date, the exposure was accumulated using a best-estimate rodded depletion analysis to End of Full Power Life (EOFPL) followed by a projected coastdown to End of Cycle (EOC).

Table 3.3.1 gives the assumed nominal exposure on the Current Cycle and the Beginning of Cycle (BOC) core average exposure that results from the shuffle into the Reload Cycle loading pattern. The Reload Cycle EOFPL core average exposure and cycle capability are provided.

TABLE 3.1.1

Assumed VY Cycle 16 Fuel Bundle Types and Numbers

	Fuel Designation	Reload Designation	Cycle Loaded	Number of Bundles
Irradiated	BD326B	R13A	14	68
	BD324B	R13B	14	44
	BP8DWB311-10GZ	R14A	15	64
	BP8DWB311-11GZ	R14B	15	64
New	BP8DWB311-10GZ	R15A	16	40
	BP8DWB311-11GZ	R15B	16	88

TABLE 3.3.1

Design Basis VY Cycle 15 and Cycle 16 Exposures*

Assumed End of Current Cycle Core Average Exposure with an Exposure Window of ± 600 MWd/St[5]	20.87±.6 GWd/St
Assumed Beginning of Reload Cycle Core Average Exposure	11.22 GWd/St
Haling Calculated End of Full Power Life Reload Cycle Core Average Exposure	20.46 GWd/St
Reload Cycle Full Power Exposure Capability	9.24 GWd/St

* According to SIMULATE-3.

Row	23	25	27	29	31	33	35	37	39	41	43
22	R13B 20.376	R15B 0.000	R13B 20.614	R15B 0.000	R13A 21.255	R15B 0.000	R13A 21.947	R15B 0.000	R14A 11.108	R14A 12.758	R13A 22.482
20	R15B 0.000	R14A 9.066	R15B 0.000	R14A 11.307	R15B 0.000	R14B 12.102	R15B 0.000	R14B 12.710	R15A 0.000	R14A 12.982	R13B 22.885
18	R13B 20.672	R15B 0.000	R13B 20.431	R15B 0.000	R13A 21.863	R15B 0.000	R14A 13.213	R15A 0.000	R14A 12.94[illegible]	R14A 13.094	R13B 25.489
16	R15B 0.000	R14A 11.297	R15B 0.000	R14A 9.104	R15B 0.000	R14B 12.285	R15A 0.000	R15A 0.000	R14B 12.923	R13B 23.608	
14	R13A 21.047	R15B 0.000	R13A 21.967	R15B 0.000	R13A 22.313	R15B 0.000	R14B 12.691	R14B 12.645	R13A 22.471		
12	R15B 0.000	R14B 12.062	R15B 0.000	R14B 12.298	R15B 0.000	R14B 12.467	R15A 0.000	R14B 12.877	R13B 22.599		
10	R13A 22.159	R15B 0.000	R14A 13.246	R15A 0.000	R14B 12.590	R15A 0.000	R14B 12.520	R13A 22.026	R13A 25.379		
08	R15B 0.000	R14B 12.674	R15A 0.000	R15A 0.000	R14B 12.661	R14B 12.850	R13A 21.923	R13A 25.202			
06	R14A 11.135	R15A 0.000	R14A 12.791	R14B 12.963	R13A 22.433	R13A 23.095	R13B 25.430				
04	R14A 12.809	R14A 12.861	R14A 13.079	R13B 23.535							
02	R13A 22.504	R13A 22.635	R13B 25.476								

.... BUNDLE ID

.... BOC EXPOSURE (GWD/ST)

BUNDLE ID	FUEL DESIGNATION
R13A	BD326B
R13B	BD324B
R14A	BP8DWB311-10GZ
R14B	BP8DWB311-11GZ
R15A	BP8DWB311-10GZ
R15B	BP8DWB311-11GZ

FIGURE 3.2.1

VY Cycle 16 Design Reference Loading Pattern, Lower Right Quadrant

WPP40/10

4.0 FUEL MECHANICAL AND THERMAL DESIGN

4.1 Mechanical Design

Most of the fuel to be inserted into the Reload Cycle was fabricated by GE. The major mechanical design parameters are given in Table 4.1.1 and Reference 2. Detailed descriptions of the fuel rod mechanical design and mechanical design analyses are provided in Reference 2. These design analyses remain valid with respect to the Reload Cycle operation. Mechanical and chemical compatibility of the fuel bundles with the in-service reactor environment is also addressed in Reference 2.

4.2 Thermal Design

The fuel thermal effects calculations were performed using the FROSSTEY-2 computer code[6]. The FROSSTEY-2 code calculates pellet-to-cladding gap conductance and fuel temperatures from a combination of theoretical and empirical models which include fuel and cladding thermal expansion, fission gas release, pellet swelling, pellet densification, pellet cracking, and fuel and cladding thermal conductivity.

The thermal effects analysis included the calculation of fuel temperatures and fuel cladding gap conductance under nominal core steady state and peak linear heat generation rate conditions. Figure 4.2.1 provides the core average response of gap conductance. These calculations integrate the responses of individual fuel batch average operating histories over the core average exposure range of the Reload Cycle. The gap conductance values are weighted axially by power distributions and radially by volume. The core-wide gap conductance values for the RETRAN system simulations, described in Sections 7.1 through 7.3, are from this data set at the corresponding exposure statepoints.

The gap conductance values input to the hot channel calculations (Section 7.1) were evaluated for the limiting fuel bundle type as a function of the assembly exposure. The calculation assumed a 1.4

chopped cosine axial power shape with the peak power node running at the maximum average planar linear heat generation rate (MAPLHGR) limits[7]. Figure 4.2.2 provides the hot channel response of gap conductance for the limiting bundle type. In Figure 4.2.2, "planar exposure" refers to the exposure of the node operating at the MAPLHGR limits. Gap conductance values for the hot channel analysis were extracted from the figures using the limiting bundle exposure of any minimum critical power ratio (MCPR) limiting bundle within the exposure interval of interest. The SIMULATE rodded depletion (Section 5.1.2) provides predictions of both limiting MCPR and the associated bundle exposure for the entire cycle.

Table 4.2.1 provides the core average and hot channel gap conductance values used in the transient analyses (Section 7.1). Fuel rod local linear heat generation rates (LHGR) at fuel centerline incipient melt and 1% cladding plastic strain as a function of local axial segment exposure for the peak gadolinia concentrations used in the Vermont Yankee fuel bundles are shown in Table 4.2.2. Initial conditions assumed that fuel rods operated at the local segment power level of the maximum allowable LHGR prior to the power increase.

4.3 Operating Experience

All irradiated fuel bundles scheduled to be reinserted in the Reload Cycle have operated as expected in Past Cycles of Vermont Yankee. Off-gas measurements in the Current Cycle indicate that a fuel rod failure has occurred. Vermont Yankee is planning to identify and discharge the failed rod(s) during the outage.

TABLE 4.1.1

Nominal Fuel Mechanical Design Parameters

	Irradiated Fuel Types		New Fuel Type
Fuel Bundle*	Twice-Burned	Once-Burned	
Bundle Types	BP8X8EB	GE8X8NB	GE8X8NB
Vendor Designation	BD324B & BD326B	BP8DWB311-10GZ & BP8DWB311-11GZ	BP8DWB311-10GZ & BP8DWB311-11GZ
Initial Enrichment, w/o U_{235}	3.24 & 3.26	3.11	3.11
Rod Array	8X8	8X8	8X8
Fuel Rods per Bundle	60	60	60
Outer Fuel Channel			
Material	Zr-4	Zr-2	Zr-2
Wall Thickness, inches	0.080	0.080	0.080

* Complete bundle, rod, and pellet descriptions are found in Reference 2.

TABLE 4.2.1

VY Cycle 16 Gap Conductance Values Used in Transient Analyses

Cycle Exposure Statepoint	Core Average Gap Conductance ($BTU/Hr-Ft^2-°F$)	Hot Channel Bundle Exposure (MWd/St)	Hot Channel Gap Conductance* ($BTU/Hr-Ft^2-°F$)
BOC	3120	7930	4900
EOFPL-2000 MWd/St	4670	8576	5010
EOFPL-1000 MWd/St	4890	10005**	5080**
EOFPL	5000	10005**	5080**

* Hot channel gap conductance values are derived for the BP8DWB311-10GZ fuel type because it is conservative compared to the other fuel types.

** Corresponding to the maximum encountered in the exposure range.

TABLE 4.2.2

Peak Linear Heat Generation Rates Corresponding to Incipient Fuel Centerline Melting and 1% Cladding Plastic Strain*

Fuel Type GE8X8EB	Exposure (MWd/St)	0.0 w/o Gd_2O_3 Melt (kW/ft)	0.0 w/o Gd_2O_3 1% ϵ_p (kW/ft)	[illegible].0 w/o Gd_2O_3 Melt (kW/ft)	[illegible].0 w/o Gd_2O_3 1% ϵ_p (kW/ft)
BD324B	0	24.0	24.0	21.0	23.0
and	35,000	24.0	24.0	20.0	20.0
BD326B	60,000	24.0	16.0	19.0	12.0

Fuel Type GE8X8NB	Exposure (MWd/St)	0.0 w/o Gd_2O_3 Melt (kW/ft)	0.0 w/o Gd_2O_3 1% ϵ_p (kW/ft)	4.0 w/o Gd_2O_3 Melt (kW/ft)	4.0 w/o Gd_2O_3 1% ϵ_p (kW/ft)
BP8DWB311-11GZ	0	24.0	24.0	21.0	23.5
and	25,000	24.0	24.0	20.0	20.0
BP8DWB311-10GZ	50,000	20.5	13.5	16.5	11.0

* Peak linear heat generation rates shown are minimum bounding values to the occurrence of the given condition.

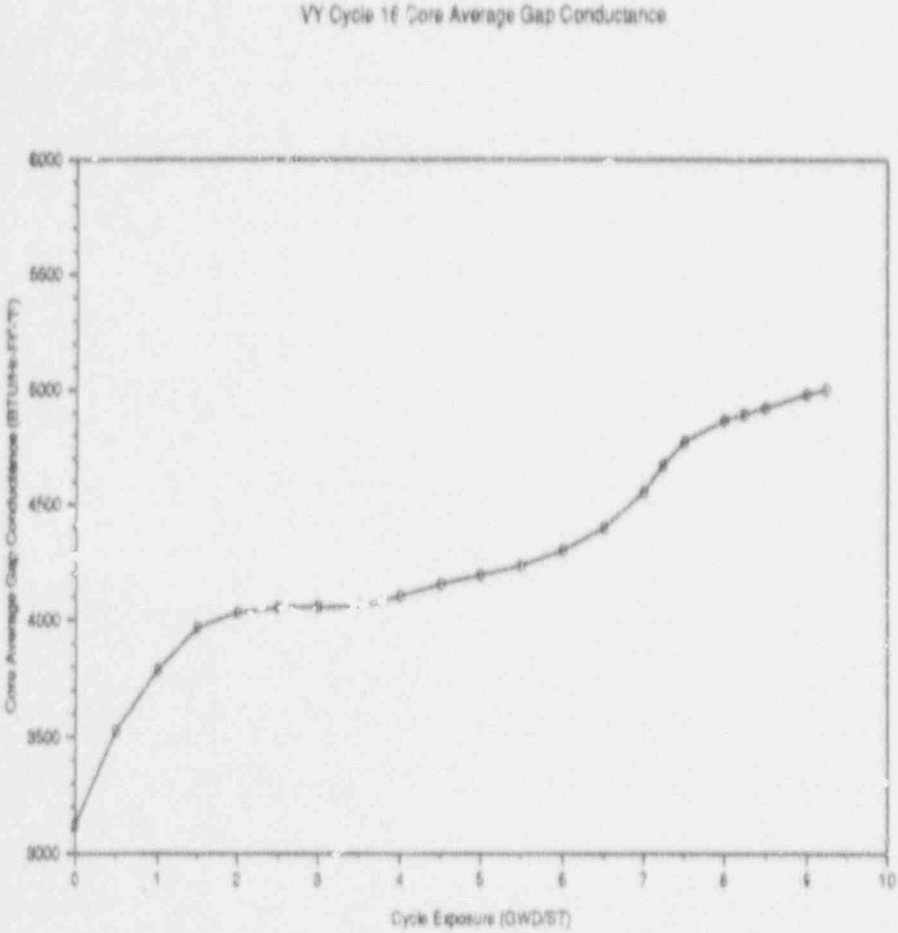

FIGURE 4.2.1

VY Cycle 16 Core Average Gap Conductance Versus Cycle Exposure

VY Hot Channel Gap Conductance for GE8x8NB

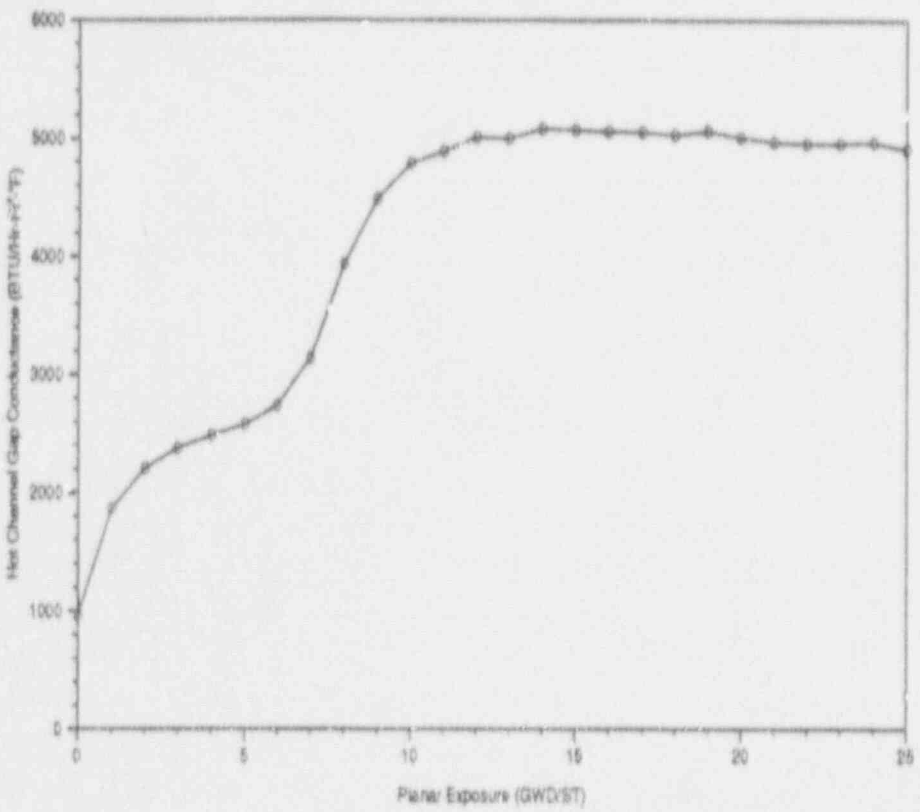

FIGURE 4.2.2

VY Hot Channel Gap Conductance for GE8X8NB Versus Exposure

5.0 NUCLEAR DESIGN

5.1 Core Power Distributions

The Reload Cycle was depleted using SIMULATE-3 to give both a rodded depletion and an All Rods Out (ARO) Haling depletion.

5.1.1 Haling Power Distribution

The Haling depletion serves as the basis for defining core reactivity characteristics for most transient evaluations. This is primarily because its flat power shape has conservatively weak scram characteristics.

The Haling power distribution is calculated in the ARO condition. The Haling iteration converges on a self-consistent power and exposure distribution for the burnup step to EOFPL. In principle, this should provide the overall minimum peaking power shape for the cycle. During the actual cycle, flatter power distributions might occasionally be achieved by shaping with control rods. However, such shaping would leave underburned regions in the core which would peak at another point in time. Figures 5.1.1 and 5.1.2 give the Haling radial and axial average power distributions for the Reload Cycle.

5.1.2 Rodded Depletion Power Distribution

The rodded depletion was used to evaluate the mislocated bundle error and the rod withdrawal error because it provides the initial rod patterns and more realistic predictions of initial CPR values. It was also used in the rod drop worth and shutdown margin calculations because it burns the top of the core more realistically than the Haling depletion. The rodded depletion also provides the hot channel bundle exposures for the gap conductance calculation.

To generate the rodded depletion, control rod patterns were developed which give critical eigenvalues at several points in the cycle and peaking similar to the Haling calculation. The resulting patterns were frequently more peaked than the Haling, but were below expected operating limits. However, as stated above, the underburned regions of the core can exhibit peaking in excess of the Haling peaking when pulling ARO at EOFPL. Figures 5.1.3 and 5.1.4 give the ARO at EOFPL power distributions for the Reload Cycle rodded depletion. Note, in Figure 5.1.4, that the average axial power at ARO for the rodded depletion is more bottom peaked than the Haling (Figure 5.1.2). The rodded depletion would result in better scram characteristics at EOFPL.

5.2 Core Exposure Distributions

The Reload Cycle exposures are summarized in Table 3.3.1. The projected BOC radial exposure distribution for the Reload Cycle is given in Figure 3.2.1. The Haling calculation produced the EOFPL radial exposure distribution given in Figure 5.2.1. Since the Haling power shape is constant, it can be held fixed by SIMULATE-3 to give the exposure distributions at various mid-cycle points. BOC, EOFPL-2000 MWd/St, EOFPL-1000 MWd/St, and EOFPL exposure distributions were used to develop reactivity input for the core wide transient analyses.

The rodded depletion differs from the Haling during the cycle because the rods shape the power differently. However, rod sequences are swapped frequently and the overall exposure distribution at end of cycle is similar to the Haling. Figure 5.2.2 gives the EOFPL radial exposure distribution for the Reload Cycle rodded depletion.

5.3 Cold Shutdown Margin

Technical Specifications[8] state that, for sufficient shutdown margin, the core must be subcritical by at least 0.25% ΔK + R (defined below) with the strongest worth control rod withdrawn. Using SIMULATE-3, a search was made for the strongest worth control rod at various exposures in the cycle. This is necessary because rod worths change with exposure on adjacent assemblies. Then the cold K_{eff} with the strongest rod out was calculated at BOC and at the end of each control rod sequence. Subtracting each cold K_{eff} with the strongest rod out from the cold critical K_{eff} defines the shutdown margin as a function of exposure. Figure 5.3.1 shows the results.

The cold critical K_{eff} was defined as the average calculated critical K_{eff} minus a 95% confidence level uncertainty. Then all cold results were normalized to make the critical K_{eff} equal to 1.000.

Because the local reactivity may increase with exposure, the shutdown margin (SDM) may decrease. To account for this and other uncertainties, the value R is calculated. R is defined as R_1 plus R_2. R_1 is the difference between the cold K_{eff} with the strongest rod out at BOC and the maximum cold K_{eff} with the strongest rod out in the cycle. R_2 is a measurement uncertainty in the demonstration of SDM associated with the manufacture of past control blades. It is presently set at .07% ΔK. The shutdown margin results are summarized in Table 5.3.1.

5.4 Maximum K_∞ for the Spent Fuel Pool

Section 5.5E of the Technical Specifications requires that the K_∞ for any bundle stored in either the new fuel vault or the spent fuel pool not exceed 1.31 to ensure compliance with the K_{eff} safety limit of 0.95. The bundles used in the Reload Cycle do not exceed the specifications in Section 5.5E, as shown in Table 5.4.1. These values are obtained from CASMO-3G[9].

TABLE 5.3.1

VY Cycle 16 K_{eff} Values and Shutdown Margin Calculation

Cold Critical K_{eff}	1.0000
BOC K_{eff} - Controlled With Strongest Worth Rod Withdrawn	.9849
Cycle Minimum Shutdown Margin Occurs at BOC With Strongest Worth Rod Withdrawn	1.51% ΔK
R_1, Maximum Increase in Cold K_{eff} With Exposure	0.00% ΔK

TABLE 5.4.1

VY Cycle 16 Maximum Cold K_∞ of any Enriched Segment

Bundle Type	Maximum K_∞
BD324B	1.20
BD326B	1.20
BP8DWB311-10GZ	1.20
BP8DWB311-11GZ	1.20

	23	25	27	29	31	33	35	37	39	41	43
22	R13B 1.110	R15B 1.392	R13B 1.146	R15B 1.393	R13A 1.118	R15B 1.347	R13A 1.061	R15B 1.235	R14A 0.989	R14A 0.762	R13A 0.434
20	R15B 1.391	R14A 1.288	R15B 1.411	R14A 1.254	R15B 1.383	R14B 1.204	R15B 1.311	R14B 1.083	R15A 1.077	R14A 0.733	R13B 0.403
18	R13B 1.144	R15B 1.411	R13B 1.152	R15B 1.400	R13A 1.116	R15B 1.351	R14A 1.144	R15A 1.192	R14A 0.902	R14A 0.654	R13B 0.349
16	R15B 1.393	R14A 1.254	R15B 1.401	R14A 1.271	R15B 1.364	R14B 1.175	R15A 1.254	R15A 1.113	R14B 0.786	R13B 0.456	
14	R13A 1.121	R15B 1.383	R13A 1.116	R15B 1.365	R13A 1.071	R15B 1.276	R14B 1.050	R14B 0.888	R13A 0.578		
12	R15B 1.347	R14B 1.205	R15B 1.352	R14B 1.176	R15B 1.277	R14B 1.067	R15A 1.072	R14B 0.754	R13B 0.446		
10	R13A 1.049	R15B 1.311	R14A 1.143	R15A 1.254	R14B 1.052	R15A 1.073	R14B 0.823	R13A 0.551	R13A 0.332		
08	R15B 1.234	R14B 1.083	R15A 1.192	R15A 1.114	R14B 0.888	R14B 0.753	R13A 0.552	R13A 0.354			
06	R14A 0.988	R15A 1.077	R14A 0.904	R14B 0.786	R13A 0.578	R13A 0.444	R13B 0.332				
04	R14A 0.761	R14A 0.73[illegible]	R14A 0.655	R13B 0.457							
02	R13A 0.433	R13A 0.402	R13B 0.350								

.... BUNDLE ID

.... EOFPL RELATIVE POWER

BUNDLE ID	FUEL DESIGNATION
R13A	BD326B
R13B	BD324B
R14A	BP8DWB311-10GZ
R14B	BP8DWB311-11GZ
R15A	BP8DWB311-10GZ
R15B	BP8DWB311-11GZ

FIGURE 5.1.1

VY Cycle 16 Haling Depletion, EOFPL Bundle Average Relative Powers

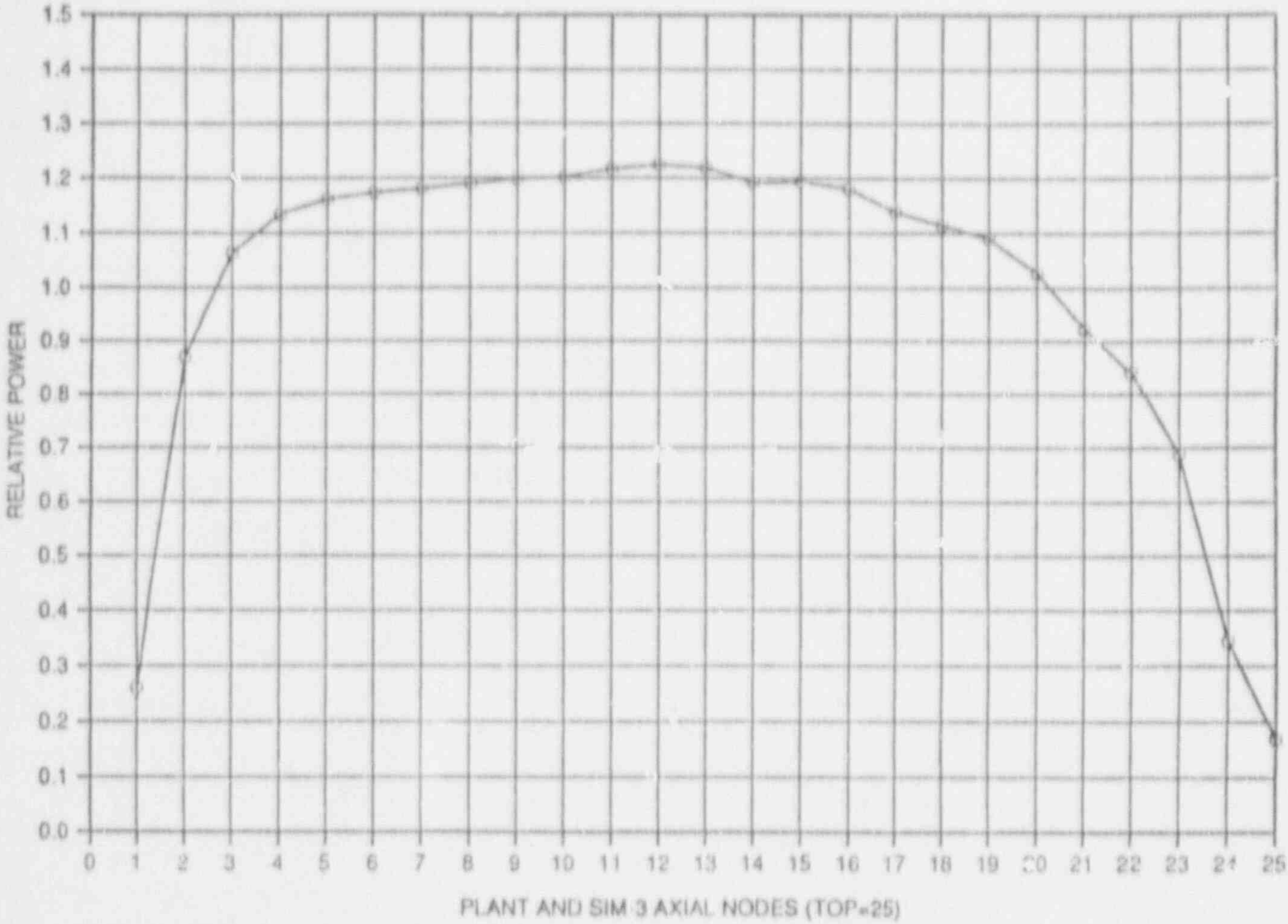

FIGURE 5.1.2

VY Cycle 16 Haling Depletion, EOFPL Core Average Axial Power Distribution

WPP40/10

	23	25	27	29	31	33	35	37	39	41	43
22	R13B 1.094	R15B 1.348	R13B 1.121	R15B 1.401	R13A 1.148	R15B 1.385	R13A 1.076	R15B 1.242	R14A 0.986	R14A 0.752	R13A 0.430
20	R15B 1.352	R14A 1.068	R15B 1.188	R14A 1.247	R15B 1.417	R14B 1.225	R15B 1.328	R14B 1.087	R15A 1.073	R14A 0.724	R13B 0.309
18	R13B 1.126	R15B 1.190	R13B 0.995	R15B 1.398	R13A 1.144	R15B 1.375	R14A 1.156	R15A 1.195	R14A 0.898	R14A 0.648	R13B 0.345
16	R15B 1.410	R14A 1.254	R15B 1.402	R14A 1.286	R15B 1.39[illegible]	R14B 1.196	R15A 1.271	R15A 1.118	R14B 0.785	R13B 0.455	
14	R13A 1.159	R15B 1.425	R13A 1.149	R15B 1.400	R13A 1.100	R15B 1.303	R14B 1.061	R14B [illegible]89	R13A 0.579		
12	R15B 1.402	R14B 1.235	R15B 1.385	R14B 1.203	R15B 1.307	R14B 1.084	R15A 1.087	R14B 0.756	R13B 0.447		
10	R13A 1.085	R15B 1.340	R14A 1.162	R15A 1.279	R14B 1.068	R15A 1.089	R14B 0.831	R13A 0.554	R13A 0.334		
08	R15B 1.253	R14B 1.095	R15A 1.203	R15A 1.124	R14B 0.893	R14B 0.759	R13A 0.555	R13A 0.356			
06	R14A 0.992	R15A 1.080	R14A 0.905	R14B 0.789	R13A 0.581	R13A 0.446	R13B 0.333				
04	R14A 0.755	R14A 0.729	R14A 0.652	R13B 0.457							
02	R13A 0.431	R13A 0.400	R13B 0.346								

.... BUNDLE ID

.... EOFPL RELATIVE POWER

BUNDLE ID	FUEL DESIGNATION
R13A	BD326B
R13B	BD324B
R14A	BP8DWB311-10GZ
R14B	BP8DWB311-11GZ
R15A	BP8DWB311-10GZ
R15B	BP8DWB311-11GZ

FIGURE 5.1.3

VY Cycle 16 Rodded Depletion - ARO at EOFPL, Bundle Average Relative Powers

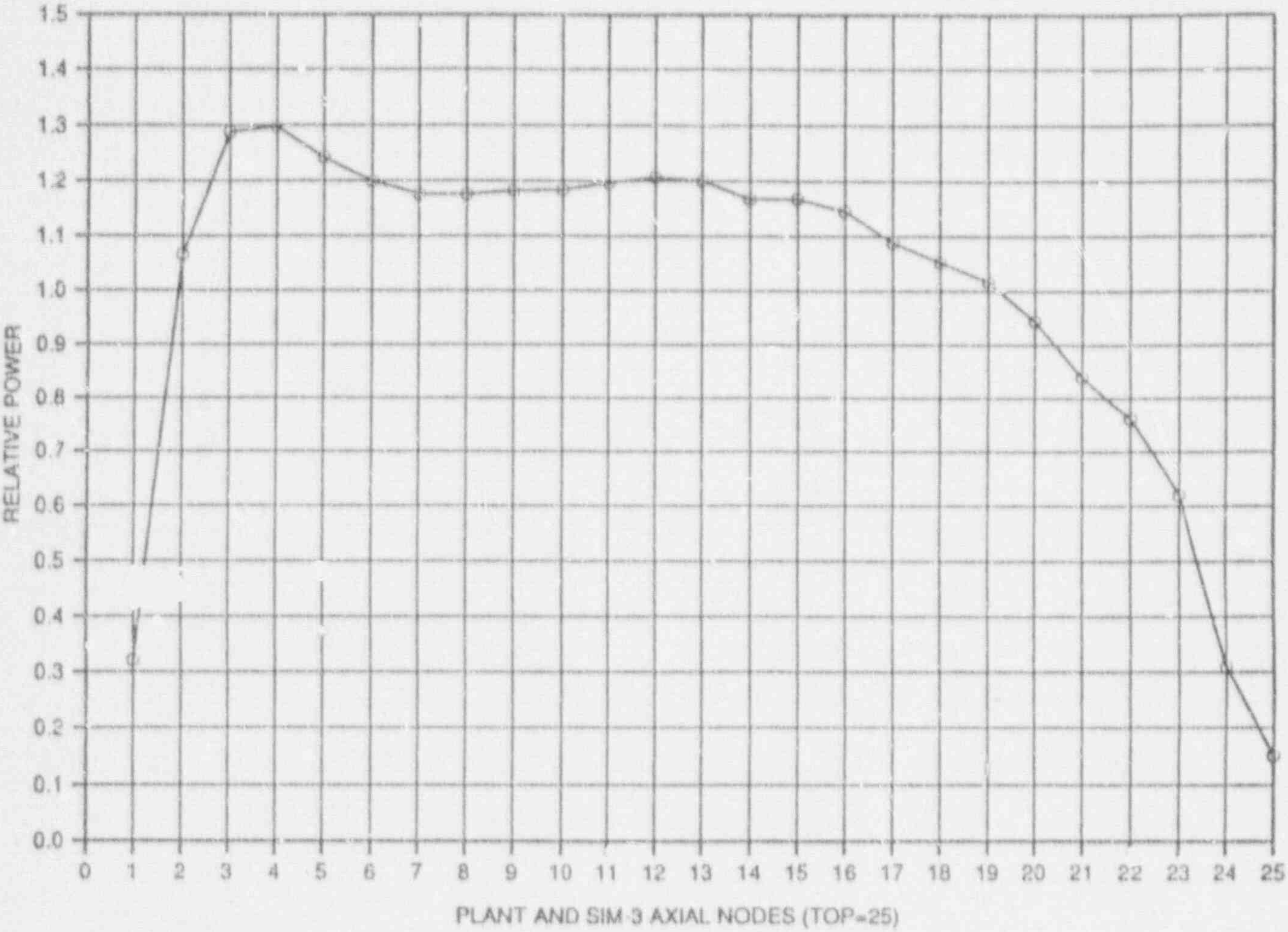

FIGURE 5.1.4

VY Cycle 16 Rodded Depletion - ARO at EOFPL,
Core Average Axial Power Distribution

	23	25	27	29	31	33	35	37	39	41	43
22	R13B 30.637	R15B 12.794	R13B 31.198	R15B 12.801	R13A 31.542	R15B 12.380	R13A 31.625	R15B 11.344	R14A 20.192	R14A 19.755	R13A 26.476
20	R15B 12.781	R14A 20.894	R15B 12.968	R14A 22.824	R15B 12.707	R14B 23.171	R15B 12.044	R14B 22.658	R15A 9.889	R14A 19.715	R13B 26.608
18	R13B 31.238	R15B 12.965	R13B 31.077	R15B 12.867	R13A 32.139	R15B 12.416	R14A 23.716	R15A 10.940	R14A 21.225	R14A 19.105	R13B 28.716
16	R15B 12.802	R14A 22.819	R15B 12.875	R14A 20.774	R15B 12.532	R14B 23.086	R15A 11.515	R15A 10.222	R14B 20.150	R13B 27.824	
14	R13A 31.362	R15B 12.712	R13A 32.241	R15B 12.539	R13A 32.168	R15B 11.728	R14B 22.340	R14B 20.803	R13A 27.786		
12	R15B 12.380	R14B 23.140	R15B 12.420	R14B 23.103	R15B 11.730	R14B 22.271	R15A 9.846	R14B 19.802	R13B 27.017		
10	R13A 31.810	R15B 12.042	R14A 23.744	R15A 11.518	R14B 22.256	R15A 9.847	R14B 20.084	R13A 27.101	R13A 28.440		
08	R15B 11.337	R14B 22.625	R15A 10.941	R15A 10.223	R14B 20.818	R14B 19.773	R13A 27.005	R13A 28.457			
06	R14A 20.209	R15A 9.888	R14A 21.090	R14B 20.187	R13A 27.752	R13A 27.182	R13B 28.500				
04	R14A 19.793	R14A 19.602	R14A 19.094	R13B 27.755							
02	R13A 29.491	R13A 26.338	R13B 28.709								

...... BUNDLE ID

...... EOFPL EXPOSURE (GWD/ST)

BUNDLE ID	FUEL DESIGNATION
R13A	BD326B
R13B	BD324B
R14A	BP8DWB311-10GZ
R14B	BP8DWB311-11GZ
R15A	BP8DWB311-10GZ
R15B	BP8DWB311-11GZ

FIGURE 5.2.1

VY Cycle 16 Haling Depletion, EOFPL Bundle Average Exposures

WPP40/10

	23	25	27	29	31	33	35	37	39	41	43
22	R13B 29.287	R15B 10.473	R13B 30.095	R15B 11.027	R13A 31.038	R15B 11.756	R13A 31.988	R15B 11.569	R14A 21.170	R14A 20.751	R13A 27.173
20	R15B 10.329	R14A 19.555	R15B 10.987	R14A 22.037	R15B 11.499	R14B 23.542	R15B 12.134	R14B 23.539	R15A 10.387	R14A 20.630	R13B 27.246
18	R13B 29.999	R15B 10.926	R13B 30.201	R15B 11.412	R13A 31.852	R15B 12.249	R14A 24.418	R15A 11.272	R14A 22.159	R14A 19.951	R13B 29.310
16	R15B 10.879	R14A 21.920	R15B 11.338	R14A 20.482	R15B 11.840	R14B 23.513	R15A 11.566	R15A 10.475	R14B 20.974	R13B 28.448	
14	R13A 30.701	R15B 11.327	R13A 31.852	R15B 11.790	R13A 32.276	R15B 11.543	R14B 22.967	R14B 21.586	R13A 28.463		
12	R15B 11.366	R14B 23.341	R15B 12.108	R14B 23.400	R15B 11.441	R14B 22.717	R15A 9.830	R14B 20.476	R13B 27.562		
10	R13A 31.879	R15B 11.942	R14A 24.317	R15A 11.401	R14B 22.768	R15A 9.793	R14B 20.629	R13A 27.660	R13A 28.891		
08	R15B 11.375	R14B 23.365	R15A 11.136	R15A 10.370	R14B 21.533	R14B 20.418	R13A 27.553	R13A 28.880			
06	R14A 21.074	R15A 10.261	R14A 21.929	R14B 20.940	R13A 28.382	R13A 27.696	R13B 28.946				
04	R14A 20.713	R14A 20.448	R14A 19.881	R13B 28.338							
02	R13A 27.144	R13A 26.933	R13B 29.267								

...... BUNDLE ID

...... EOFPL EXPOSURE (GWD/ST)

BUNDLE ID	FUEL DESIGNATION
R13A	BD326B
R13B	BD324B
R14A	BP8DWB311-10GZ
R14B	BP8DWB311-11GZ
R15A	BP8DWB311-10GZ
R15B	BP8DWB311-11GZ

FIGURE 5.2.2

VY Cycle 16 Rodded Depletion, EOFPL Bundle Average Exposures

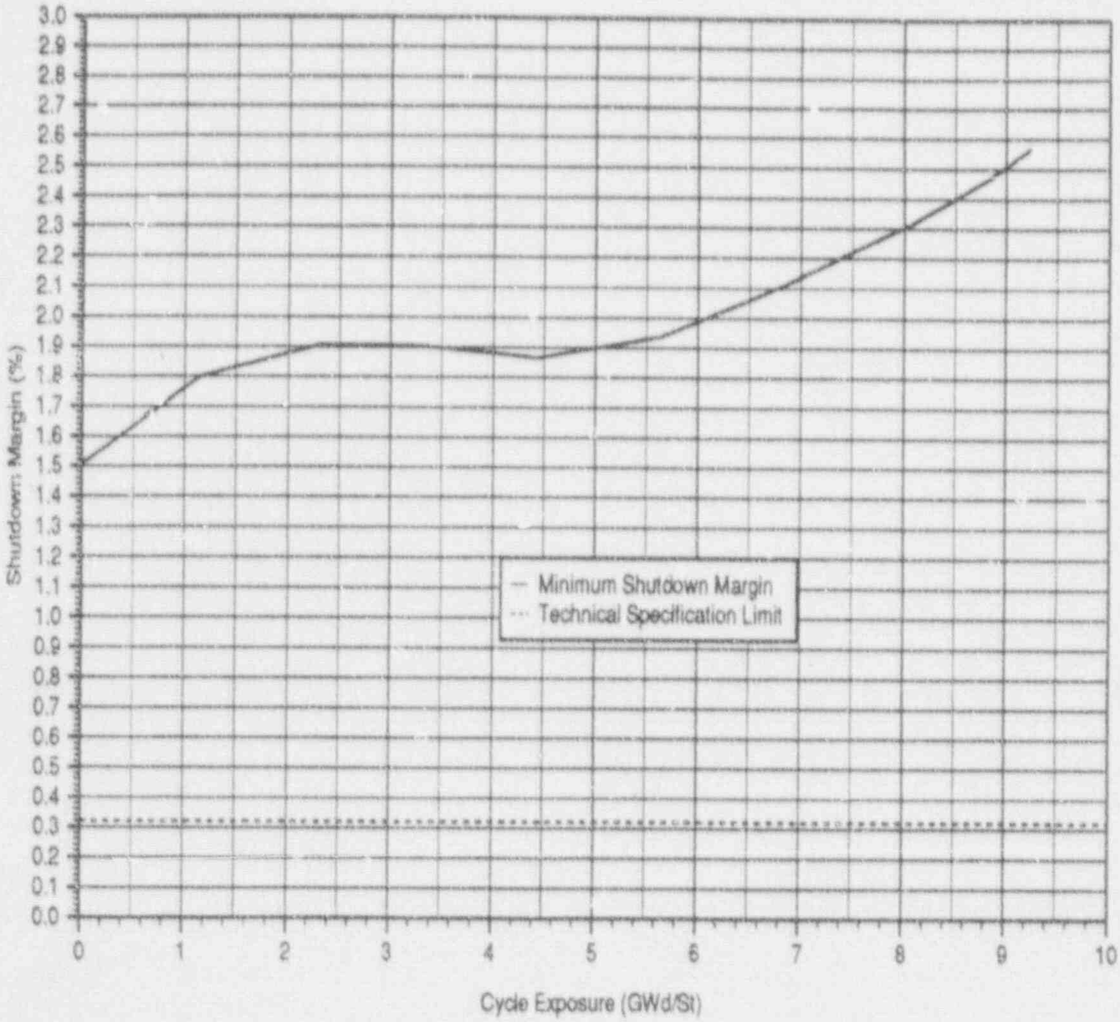

FIGURE 5.3.1

VY Cycle 16 Cold Shutdown ΔK in Percent Versus Cycle Exposure

6.0 THERMAL-HYDRAULIC DESIGN

6.1 Steady-State Thermal Hydraulics

Core steady-state thermal-hydraulic analyses for the Reload Cycle were performed using the FIBWR[10],[11],[12] computer code. The FIBWR code incorporates a detailed geometrical representation of the complex flow paths in a BWR core, and explicitly models the leakage flow to the bypass region and water rod flow. The FIBWR geometric models for each GE bundle type were benchmarked against vendor-supplied and plant thermal-hydraulic information.

Using the fuel bundle geometric models, a power distribution calculated by SIMULATE-3 and core inlet enthalpy, the FIBWR code calculates the core pressure drop and total bypass flow for a given total core flow. The core pressure drop and total bypass flow predicted by the FIBWR code were then used in setting the initial conditions for the system transient analysis model.

6.2 Reactor Limits Determination

The objective for normal operation and anticipated transient events is to maintain nucleate boiling. Avoiding a transition to film boiling protects the fuel cladding integrity. The Fuel Cladding Integrity Safety Limit (FCISL) for Vermont Yankee is a Critical Power Ratio (CPR) of 1.07 [2]. CPR is defined as the ratio of the critical power (bundle power at which some point within the assembly experiences onset of boiling transition) to the operating bundle power. Thermal margin is stated in terms of the minimum value of the Minimum Critical Power Ratio (MCPR) which corresponds to the most limiting fuel assembly in the core. Both the transient (safety) and normal operating thermal limits, in terms of MCPR, are derived with the GEXL-Plus correlation[13], with appropriate coefficients representative of the Reload Cycle's hot assembly fuel type.

The Reload Cycle fuel has a Linear Heat Generation Rate (LHGR) limit of 14.4 kW/ft for all bundle types. The basis for the Maximum LHGR (MLHGR) limit can be found in Reference 2.

The Reload Cycle fuel has Average Planar Linear Heat Generation Rate (APLHGR) limits shown in Appendix A. The Maximum APLHGR (MAPLHGR) values are the most limiting composite of the fuel mechanical analysis MAPLHGRs and the LOCA analysis MAPLHGRs. The fuel mechanical design analysis, using the methods in Reference 2, demonstrate that all fuel rods in a lattice, operating at the bounding power history, meet the fuel design limits specified in Reference 2. The transients described in Section 7.0 were analyzed to verify that design criteria in the mechanical design analysis methods was not exceeded during the transient. The LOCA analysis is described in Section 8.0.

7.0 ABNORMAL OPERATIONAL TRANSIENT ANALYSIS

7.1 Pressurization Transient Analysis

Transient simulations are performed to assess the impact of certain transients on the heat transfer characteristics of the fuel. It is the purpose of the analysis to determine the MCPR operating limit, such that the FCISL is not violated for the transients considered.

7.1.1 Methodology

The analysis requires two types of simulations. A system level simulation is performed to determine the overall plant response. Transient core inlet and exit conditions and normalized power from the system level calculation are then used to perform detailed thermal-hydraulic simulations of the fuel, referred to as "hot channel calculations." The hot channel simulations provide the bundle transient ΔCPR (the initial bundle CPR minus the MCPR experienced during the transient).

The system level simulations are performed with the one dimensional (1-D) RETRAN model[14],[15],[16]. The hot channel calculations are performed with the RETRAN[17],[18] and TCPYA01[19],[11],[15] computer codes. The GEXL-Plus correlation [12] is used in TCPYA01 to evaluate critical power ratio. The calculational procedure is outlined below.

The hot channel transient ΔCPR calculations employ a two-part process, as illustrated by the flow chart in Figure 7.1.1. The first part involves a series of steady-state analyses performed with the FIBWR, RETRAN, and TCPYA01 computer codes. The FIBWR analyses utilize a one-channel model for each fuel type being analyzed, with bypass and water rod flow also modeled. The steady-state FIBWR analyses were performed at several power levels with other conditions (i.e., core pressure drop, system pressure, and core inlet enthalpy) held constant. The FIBWR code result is an active channel flow (AF) and bypass flow (BPF) for each active channel power (AP).

The FIBWR conditions for channel power, channel flow, and bypass flow were then used as input to steady-state RETRAN/TCPYA01 hot channel calculations. Other assumptions are consistent with those in the FIBWR analysis. The Initial Critical Power Ratio (ICPR) is the key result for each steady-state RETRAN/TCPYA01 analysis. These results allow for the development of functional relationships, describing AP as a function of ICPR, and AF and BPF as functions of AP for each fuel type. These relationships are used in the iterative process used during the transient calculations as described below and shown in Figure 7.1.1.

The second part iterates on the hot channel initial power level. This is necessary because the ΔCPR for a given transient varies with Initial Critical Power Ratio (ICPR). However, only the ΔCPR corresponding to a transient MCPR equal to the FCISL limit (i.e., 1.07 + ΔCPR = ICPR) is appropriate. The approximate constancy of the ΔCPR/ICPR ratio is useful in these iterations. Each iteration requires a RETRAN hot channel run to calculate the transient enthalpies, flows, pressure and saturation properties at each time step. These are required for input to the TCPYA01 code. TCPYA01 is then used to calculate a CPR at each time step during the transient, from which a transient ΔCPR is derived. The hot channel model assumes a chopped cosine axial power shape with a peak/average ratio of 1.4.

As noted in Section 6.1, analyses for the Reload Cycle included benchmarking the FIBWR model against vendor-supplied thermal-hydraulic information. Therefore, the FIBWR results of AF and BPF for a given AP and core pressure drop are passed directly to RETRAN. As shown in Figure 7.1.1, the current iterative process involves a single loop.

7.1.2 Initial Conditions and Assumptions

The initial conditions for the Reload Cycle are based on a reactor power level of 1664 MW_{th} which includes a 2% calorimetric uncertainty on the reactor power level of 1631 MW_{th}. The assumed Reload Cycle analysis reactor power bounds the current licensed power level of 1593 MW_{th}. The reactor core flow is assumed to be 100%. The core axial power distribution for each of the exposure points is based on the 3-dimensional SIMULATE-3 predictions associated with the generation of the reactivity data (Section 7.1.3). The core inlet enthalpy is set so that the amount of carryunder from the steam separators and the quality in the liquid region outside the separators is as close to zero as possible. For fast pressurization transients, this maximizes the initial pressurization rate and predicts a more severe neutron power spike. A summary of the initial operating state used for the system simulations is provided in Table 7.1.1.

Vermont Yankee operators adjust core flow during the cycle for short-term maneuvering. During this type of operation, core flow may be as low as 87% while at 100% power. To ensure the safety analysis bounds these conditions, transients are reanalyzed at the limiting exposure statepoint (limiting in terms of an increase in ΔCPR) at 1664 MW_{th} power and 87% flow. These analyses are performed at both the "Measured" and the "67B" scram times. The ΔCPR penalty (defined as the difference in ΔCPR) generated during this reanalysis is applied to the applicable transient ΔCPR results.

Assumptions specific to a particular transient are discussed in the section describing the transient. In general, the following assumptions are made for all transients:

1. Scram setpoints are at Technical Specification [7] limits.

2. Protective system logic delays are at equipment specification limits.

3. Safety/relief valve and safety valve capacities are based on Technical Specification rated values.

4. Safety/relief valve and safety valve setpoints are modeled as being at the Technical Specification upper limit. Valve responses are based on slowest specified response values.

5. Control rod drive scram speed is based on the Technical Specification limits. The analysis addresses a dual set of scram speeds, referred to as the "Measured" and the "67B"

scram times. "Measured" refers to the faster scram times given in Section 3.3.C.1.1 of the Technical Specifications. "67B" refers to the slower scram times given in Section 3.3.C.1.2 of the Technical Specifications.

7.1.3 One-Dimensional Cross Sections and Kinetics Parameters

The one-dimensional (1-D) cross sections and kinetics parameters are generated as functions of fuel temperature, moderator density, and scram. The method[20] is outlined below.

A complete set of 1-D cross sections, 1-D kinetics parameters, the axial power distribution, and the kinetics parameters are generated from base states established for EOFPL, EOFPL-1000 MWd/St, EOFPL-2000 MWd/St, and BOC exposure statepoints. These statepoints are characterized by exposure and void history distributions, control rod patterns, and core thermal-hydraulic conditions. The latter are consistent with the assumed system transient conditions provided in Table 7.1.1.

The BOC base state is established by shuffling from the previously defined Current Cycle endpoint into the Reload Cycle loading pattern. A criticality search provides an estimate of the BOC critical rod pattern. The EOFPL and intermediate core exposure and void history distributions are calculated with a Haling depletion as described in Section 5.2. The EOFPL state is unrodded. As such, it is defined sufficiently. However, the EOFPL-1000 MWd/St and EOFPL-2000 MWd/St exposure statepoints require base control rod patterns. These are developed to be as "black and white" as possible. That is, beginning with the rodded depletion configuration, all control rods which are more than half inserted are fully inserted, and all control rods which are less than half inserted are fully withdrawn. If the SIMULATE-3 calculated parameters are within operating limits, then this configuration becomes the base case. If the limits are exceeded, a minimum number of control rods are adjusted a minimum number of notches until the parameters fall within limits. Using this method, the control rod patterns and resultant power distributions minimize the scram reactivity and maximize the core average moderator density reactivity coefficient. For the events analyzed, this tends to maximize the transient power response.

At each exposure statepoint, a SIMULATE-3 initial control state reference case is run. A series of perturbation cases are run with SIMULATE-3 to independently vary the fuel temperature, moderator temperature, and core pressure. All other variables normally associated with the SIMULATE-3 cross sections are held constant at the reference state. To obtain the effect of the control rod scram, another SIMULATE-3 reference case is run with all-rods-in. The perturbation cases described above are run again from this reference case. For each control state, a data set of kinetics parameters and cross sections is generated as a function of the perturbed variable. There is a table set for each of the 27 neutronic regions, 25 regions to represent the active core and one region each for the bottom and top reflectors.

7.1.4 Pressurization Transients Analyzed

Past licensing analysis has shown that the transients which result in the minimum core thermal margins are:

1. Generator load rejection with complete failure of the turbine bypass system.

2. Turbine trip with complete failure of the turbine bypass system.

3. Loss of feedwater heating.

The "feedwater controller failure" (maximum demand) transient is not a limiting transient for Vermont Yankee, because of the plant's 110% steam flow bypass system. Past analyses have shown this transient to be considerably less limiting than any of the above for all exposure points. The events reported herein are limiting; no other transients would produce more restrictive MCPR operating limits for the Reload Cycle. Brief descriptions and the results of the transients analyzed are provided in the following section.

7.2 Pressurization Transient Analysis Results

The transients selected for consideration were analyzed at exposure points of EOFPL, EOFPL-1000 MWd/St, and EOFPL-2000 MWd/St with the exception of the loss of feedwater heating transient which was evaluated at EOFPL-1000 MWd/St, EOFPL-2000 MWd/St, and BOC. The transient results reported in Table 7.2.1 correspond to the limiting bundle type in the core. The MCPR limits in Table 7.2.1 are calculated by adding the calculated ΔCPR to the FCISL. The worst ΔCPR for the pressurization transients include the 0.01 adjustment to allow for the exposure window of ±600 MWd/St on Current Cycle and the exposure uncertainty on the Reload Cycle.

7.2.1 Turbine Trip Without Bypass Transient (TTWOBP)

The transient is initiated by a rapid closure (0.1 second closing time) of the turbine stop valves. It is assumed that the steam bypass valves, which normally open to relieve pressure, remain closed. A reactor protection system signal is generated by the turbine stop valve closure switches. Control rod drive motion is conservatively assumed to occur 0.27 seconds after the start of turbine stop valve motion. The ATWS recirculation pump trip is assumed to occur at a setpoint of 1150 psig dome pressure. A pump trip time delay of 1.0 second is assumed to account for logic delay and M-G set generator field collapse. In simulating the transient, the bypass piping volume up to the valve chest is lumped into the control volume upstream of the turbine stop valves. Predictions of the salient system parameters at the three exposure points are shown in Figures 7.2.1 through 7.2.3 for the "Measured" scram time analysis.

7.2.2 Generator Load Rejection Without Bypass Transient (GLRWOBP)

The transient is initiated by a rapid closure (0.3 seconds closing time) of the turbine control valves. As in the case of the turbine trip transient, the bypass valves are assumed to fail. A reactor protection system signal is generated by the hydraulic fluid pressure switches in the acceleration relay of the turbine control system. Control rod drive motion is conservatively assumed to occur

0.28 seconds after the start of turbine control valve motion. The same modeling regarding the ATWS pump trip and bypass piping is used as in the turbine trip simulation. The influence of the accelerating main turbine generator on the recirculation system is simulated by specifying the main turbine generator electrical frequency as a function of time for the M-G set drive motors. The main turbine generator frequency curve is based on a 100% power plant startup test and is considered representative for the simulation. The system model predictions for the three exposure points are shown in Figures 7.2.4 through 7.2.6 for the "Measured" scram time analysis.

7.2.3 Loss of Feedwater Heating Transient (LOFWH)

A feedwater heater can be lost in such a way that the steam extraction line to the heater is shut off or the feedwater flow bypasses one of the heaters. In either case, the reactor will receive cooler feedwater, which will produce an increase in the core inlet subcooling, resulting in a reactor power increase.

The response of the system due to the loss of 100°F of the feedwater heating capability was analyzed. This represents the maximum expected feedwater temperature reduction for a single heater or group of heaters that can be tripped or bypassed by a single event.

Vermont Yankee has a scram setpoint of 120% of rated power as part of the Reactor Protection System (RPS) on high neutron flux. In this analysis, no credit was taken for scram on high neutron flux, thereby allowing the reactor power to reach its peak without scram. This approach was selected to provide a bounding and conservative analysis for events initiated from any power level.

The transient response of the system was evaluated at several exposures during the cycle. The transient evaluation at BOC was found to be the limiting case between BOC to EOFPL-1000 MWd/St. The results of the system response to a loss of 100°F feedwater heating capability evaluated at BOC as predicted by the RETRAN code are presented in Figure 7.2.7.

7.3 Overpressurization Analysis Results

Compliance with ASME vessel code limits is demonstrated by an analysis of the Main Steam Isolation Valves (MSIV) closing with failure of the MSIV position switch scram. EOFPL conditions were analyzed. The system model used is the same as that used for the transient analysis (Section 7.1.1). The initial conditions and modeling assumptions discussed in Section 7.1.2 are applicable to this simulation.

The transient is initiated by a simultaneous closure of all MSIVs. A 3.0 second closing time, which is the Technical Specification minimum, is assumed. A reactor scram signal is generated on APRM high flux. Control rod drive motion is conservatively assumed to occur 0.28 seconds after reaching the high flux setpoint. The system response is shown in Figure 7.3.1 for the "Measured" scram time analysis.

The maximum pressures at the bottom of the reactor vessel calculated for the "Measured" scram time analysis and for the "67B" scram time analysis are given in Table 7.3.1. These results are within the ASME code overpressure design limit which is 110% of the vessel design pressure. Vermont Yankee's design pressure is 1250 psig so the maximum pressure limit is 1375 psig.

7.4 Local Rod Withdrawal Error Transient Results

The rod withdrawal error (RWE) is a local core transient caused by an operator erroneously withdrawing a control rod in the continuous withdrawal mode. If the core is operating at its operating limits for MCPR and LHGR at the time of the error, then withdrawal of a control rod could increase both local and core power levels with the potential for overheating the fuel.

There is a broad spectrum of core conditions and control rod patterns which could be present at the time of such an error. For most normal situations it would be possible to fully withdraw a control rod without exceeding 1% clad plastic strain or violating the

FCISL.

To bound the most severe of postulated rod withdrawal error events, a portion of the core MCPR operating limit envelope is specifically defined such that the cladding limits are not violated. The consequences of the error depend on the local power increase, the initial MCPR of the neighboring locations and the ability of the Rod Block Monitor (RBM) System to stop the withdrawing rod before MCPR reaches the FCISL.

The most severe transient postulated begins with the core operating according to normal procedures and within normal operating limits. The operator makes a procedural error and attempts to fully withdraw the maximum worth control rod at maximum withdrawal speed. The core limiting locations are close to the error rod. They experience the spatial power shape transient as well as the overall core power increase.

The core conditions and control rod pattern are conservatively modeled for the bounding case by specifying the following set of concurrent worst case assumptions:

1. The rod should have high reactivity worth. This is provided for by analysis of the core at several exposure points around the core peak reactivity. The test patterns are developed with xenon-free conditions. The xenon-free condition and the additional control rod inventory needed to maintain criticality exaggerates the worth of the withdrawn control rod when compared to normal operation with normal xenon levels.

2. The core is initially at 104.5% power and 100% flow.

3. The core power distribution is adjusted with the available control rods to place the locations within the four by four array of bundles around the error rod as close to the operating limits as possible.

4. Of the many patterns tested, the pattern with the highest ΔCPR results is selected as the bounding case.

The RBM System's ability to terminate the bounding case is evaluated on the following bases:

1. Technical Specifications allow each of the separate RBM channels to remain operable if at least half of the Local Power Range Monitor (LPRM) inputs at every level are operable. For the interior RBM channels tested in this analysis, there are a maximum of four LPRM inputs per level. One RBM channel averages the inputs from the A and C levels; the other channel averages the inputs from the B and D levels. Considering the inputs for a single channel, there are eleven failure combinations of none, one and two failed LPRM strings. The RBM channel responses are evaluated separately at these eleven input failure conditions. Then, for each channel taken separately, the lowest response as a function of error rod position is chosen for comparison to the RBM setpoint.

2. The event is analyzed separately in each of the four quadrants of the core due to the differing LPRM string physical locations relative to the error rod.

Technical Specifications require that both RBM channels be operable during normal operation. Thus, the first channel calculated to intercept the RBM setpoint is assumed to stop the rod. To allow for control system delay times, the rod is assumed to move two inches after the intercept and stop at the following notch.

The analysis is performed using SIMULATE-3. Two separate cases are presented from numerous explicit SIMULATE-3 analyses. The reactor conditions and case descriptions are shown in Figures 7.4.1 and 7.4.2. Case 1 analyzes the bounding event with zero xenon at the most reactive point in the cycle for the worst case abnormal rod pattern configuration. Case 2 is the worst of the 104.5% power conditions modeled with more normal control rod patterns and equilibrium xenon.

The transient results, the ΔCPR and maximum linear heat generation rate (MLHGR) values, are also shown in Figures 7.4.1 and 7.4.2. The ΔCPR values are evaluated such that the implied MCPR operating limit equals FCISL + ΔCPR. This is done by conserving the figure of merit (ΔCPR/ICPR) shown by the SIMULATE calculations. The use of this method provides valid ΔCPR values in the analysis of normal operating states where locations near the assumed error rod are not initially near the MCPR operating limit.

Case 2 is the worst of all the rod withdrawal transients analyzed from 104.5% power, full flow and normal rod pattern conditions. Case 2 is bounded by Case 1 by at least 0.02 ΔCPR margin to assure that the exposure uncertainties on the Current Cycle and the Reload Cycle are accounted for.

The Case 1 RBM channel responses are shown in Figures 7.4.3 and 7.4.4. They also show the control rod position at the point where the weakest RBM channel response first intercepts the RBM setpoint. For this same bounding case, the operating limit ΔCPR envelope component versus RBM setpoint is taken from Figure 7.4.1. The same figure shows the resultant LHGR assuming the limiting bundle is placed on the operating limit of 14.4 kW/ft prior to the withdrawal. The limiting bundle MLHGR demonstrates margin to the 1% plastic strain limit given the low exposure of the limiting bundle. High exposure bundles which have low 1% plastic strain limits are never limiting.

7.5 Misloaded Bundle Error Analysis Results

7.5.1 Rotated Bundle Error

The primary result of a bundle rotation is a large increase in local pin peaking and R-factor as higher enrichment pins are placed adjacent to the surrounding wide water gaps. In addition, there may be a small increase in reactivity, depending on the exposure and void fraction states. The R-factor increase results in a CPR reduction, while the local pin peaking factor increase results in a higher pin LHGR. The objective of the analysis is to ensure that, in the worst possible rotation, the LHGR and CPR safety limits are not violated with the most limiting monitored bundles on their operating limits.

To analyze the CPR response, rotated bundle R-factors as a function of exposure are developed by adding the largest possible ΔR-factor resulting from a rotation to the exposure dependent R-factors of the properly oriented bundles. Using these rotated bundle R-factors, the MCPR values resulting from a bundle rotation are determined using SIMULATE. This is done for each control rod sequence throughout the cycle. The process is repeated with the K-infinity of the limiting bundle modified slightly to account for the increase in reactivity resulting from the rotation. For each sequence, the MCPR for the properly oriented bundles is adjusted by a ratio necessary to place the corresponding rotated CPR on its TCISL. The maximum of these adjusted MCPRs is the rotated bundle operating limit.

To determine the MLHGR resulting from a rotation, the ratios of the maximum rotated bundle local peaking factor to the maximum properly oriented bundle local peaking are determined for the expected range of exposure and void conditions. The maximum of this ratio is applied to the LHGR operating limit of 14.4 kW/ft. This maximum rotated bundle LHGR is, in addition, modified to account for the possible reactivity increase resulting from the rotation.

The results of the rotated bundle analysis are given in Table 7.5.1. Comparing Table 7.5.1 to Table 4.2.2, there is sufficient margin to the 1% plastic strain limit.

7.5.2 Mislocated Bundle Error

Misloading a high reactivity assembly into a region of high neutron importance results in a location of high relative assembly average power. Since the assembly is assumed to be properly oriented (not rotated), R-factors used for the misloaded bundle are the standard values for the fuel type.

The analysis uses multiple SIMULATE-3 cases to examine the effects of explicitly mislocating every older interior assembly in a quarter core with a fresh or once-burned assembly. Because of symmetry, the results apply to the whole core. Edge bundles are not examined because they are never limiting, due to neutron leakage.

The effect of the successive mislocations is examined for every control rod sequence throughout the cycle. For each sequence, the MCPR for the properly loaded core is compared to the MCPR of the misloaded core at the misloaded location. The MCPR for the properly loaded core is adjusted by a ratio necessary to place the mislocated assembly on the FCISL. The maximum of these adjusted MCPRs is the mislocated bundle operating limit.

The results of the mislocated bundle analysis are given in Table 7.5.2. Comparing Table 7.5.2 to Table 4.2.2, there is sufficient margin to the 1% plastic strain limit.

TABLE 7.1.1

VY Cycle 16 Summary of System Transient Model Initial Conditions for Transient Analyses

Core Thermal Power (MW_{th})	1664.0
Turbine Steam Flow ($10^6 lb_m/hr$)	6.75
Total Core Flow ($10^6 lb_m/hr$)	48.0
Core Bypass Flow ($10^6 lb_m/hr$)*	6.2
Core Inlet Enthalpy (BTU/lb_m)	523.2
Steam Dome Pressure (psia)	1034.7
Turbine Inlet Pressure (psia)	985.7
Total Recirculation Drive Flow ($10^6 lb_m/hr$)	23.7
Core Plate Differential Pressure (psi)	20.2
Narrow Range Water Level (in.)	162
Average Fuel Gap Conductance	(See Section 4.2)

* Includes water rod flow.

TABLE 7.2.1

VY Cycle 16 Pressurization Transient Analysis Results

Transient	Exposure Statepoint	Peak Prompt Power (Fraction of Initial Value)	Peak Average Heat Flux (Fraction of Initial Value)	ΔCPR*	Operating MCPR Limits
Turbine Trip Without Bypass, "Measured" Scram Time	EOFPL	2.954	1.213	0.14	1.21
	EOFPL-1000	1.872	1.086	0.06	1.13
	EOFPL-2000	1.211	1.000	0.02	1.09
Turbine Trip Without Bypass, "67B" Scram Time	EOFPL	3.301	1.259	0.17	1.24
	EOFPL-1000	2.2[illegible]5	1.144	0.10	1.17
	EOFPL-2000	1.605	1.049	0.05	1.12
Generator Load Rejection Without Bypass, "Measured" Scram Time	EOFPL	2.868	1.192	0.12	1.19
	EOFPL-1000	1.990	1.069	0.05	1.12
	EOFPL-2000	1.086	1.000	0.01	1.08
Generator Load Rejection Without Bypass, "67B" Scram Time	EOFPL	3.484	1.257	0.15	1.22
	EOFPL-1000	2.584	1.141	0.08	1.15
	EOFPL-2000	1.612	1.024	0.03	1.10
Loss of 100°F Feedwater Heating	EOFPL-1000	1.145	1.146	0.11	1.18
	EOFPL-2000	1.144	1.145	0.11	1.18
	BOC	1.147	1.148	0.12	1.19

* The worst ΔCPR for TTWOBP and GLRWOBP includes a 0.01 ΔCPR adjustment to allow for the exposure window of ±600 MWd/St on Current Cycle and the exposure uncertainty on the Reload Cycle.

TABLE 7.3.1

VY Cycle 16 Overpressurization Analysis Results

Conditions	Maximum Pressure at Reactor Vessel Bottom (psia)
"Measured" Scram Time	1253
"67B" Scram Time	1280

TABLE 7.5.1

VY Cycle 16 Rotated Bundle Analysis Results

Operating MCPR Limit	Maximum Attainable LHGR (kW/ft)
1.21	19.86

TABLE 7.5.2

VY Cycle 16 Mislocated Bundle Analysis Results

Operating MCPR Limit	Maximum Attainable LHGR (kW/ft)
1.17	18.09

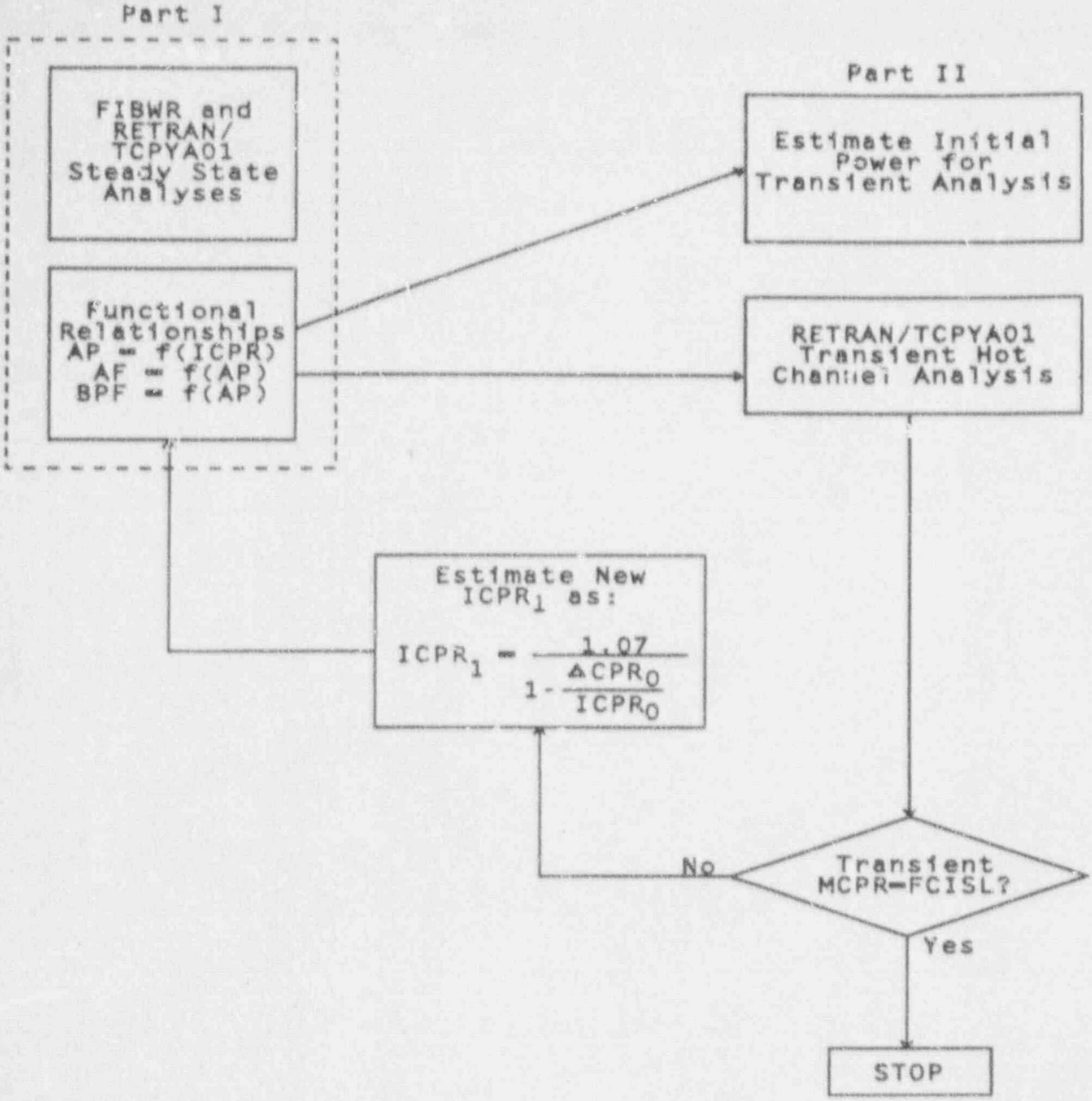

FIGURE 7.1.1

Flow Chart for the Calculation of ΔCPR Using the RETRAN/TCPYA01 Codes

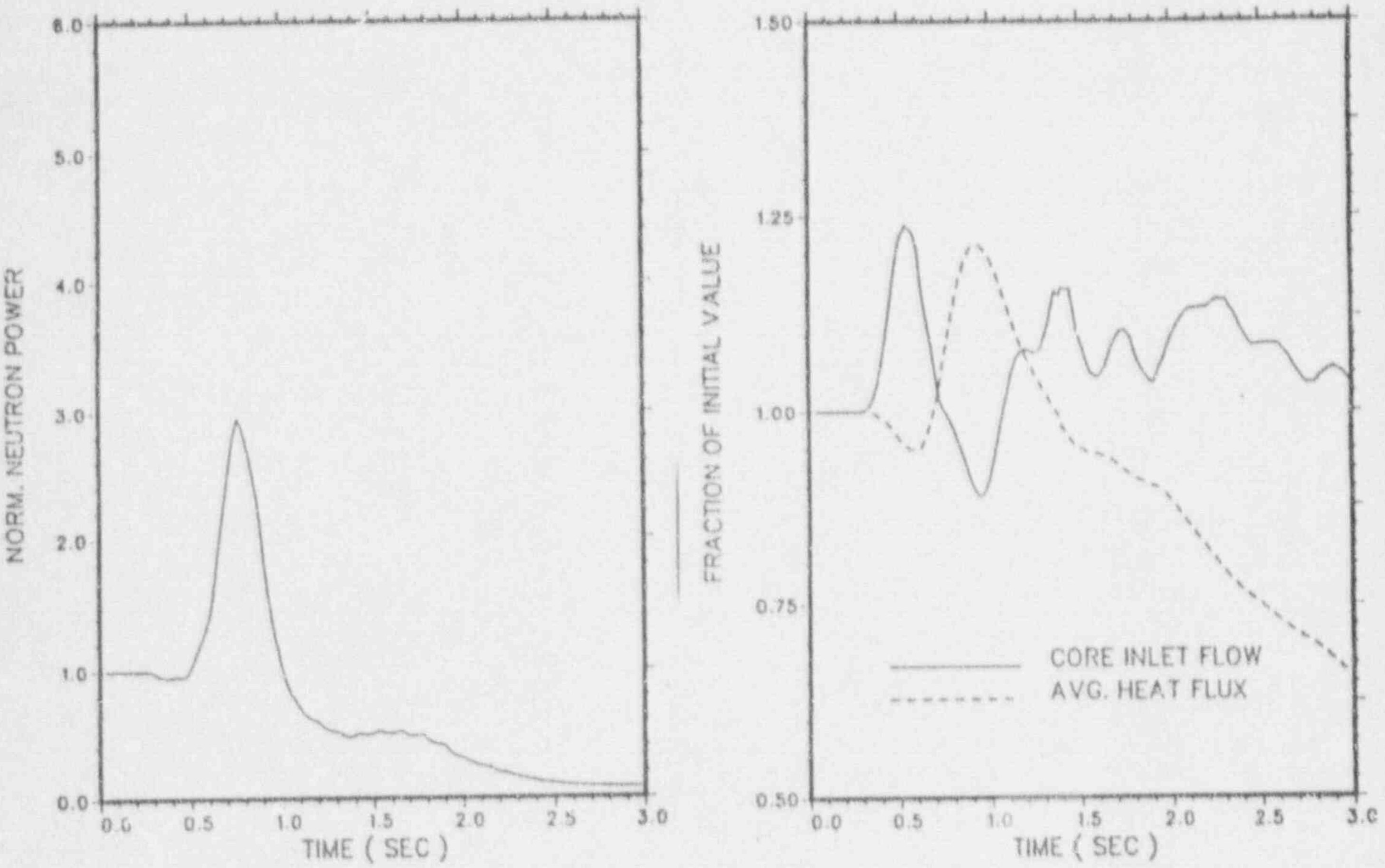

FIGURE 7.2.1

Turbine Trip Without Bypass, EOFPL16
Transient Response Versus Time, "Measured" Scram Time

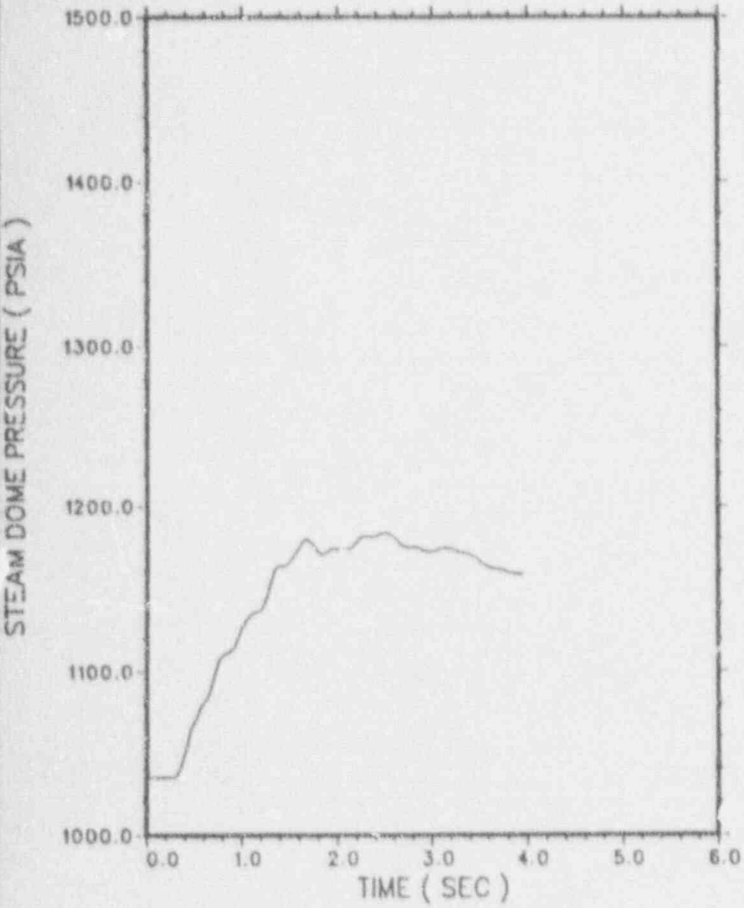

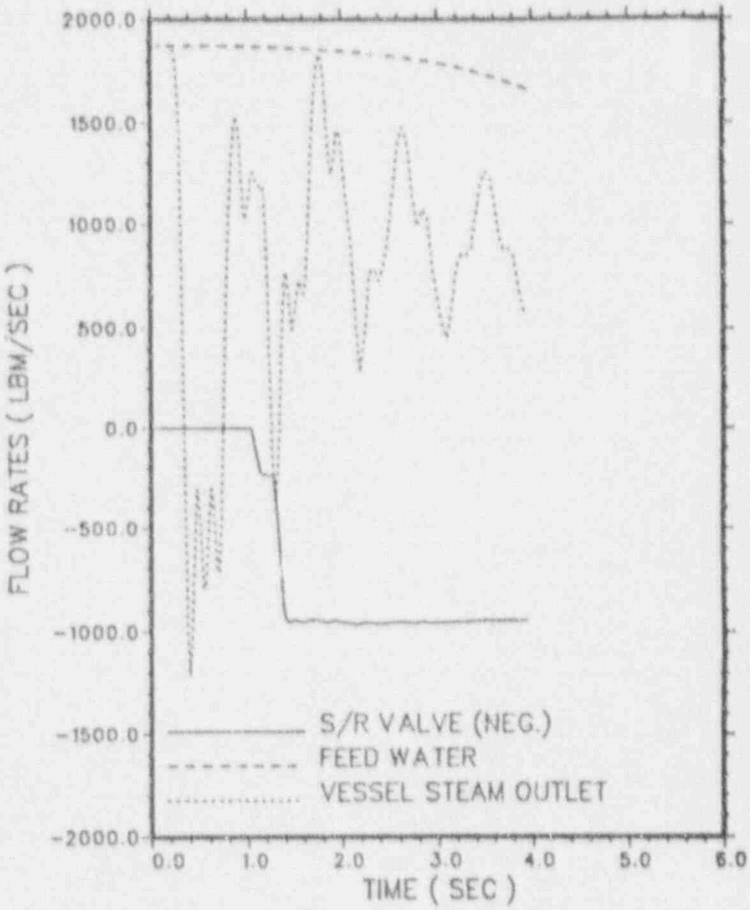

FIGURE 7.2.1
(Continued)

Turbine Trip Without Bypass, EOFPL16
Transient Response Versus Time, "Measured" Scram Time

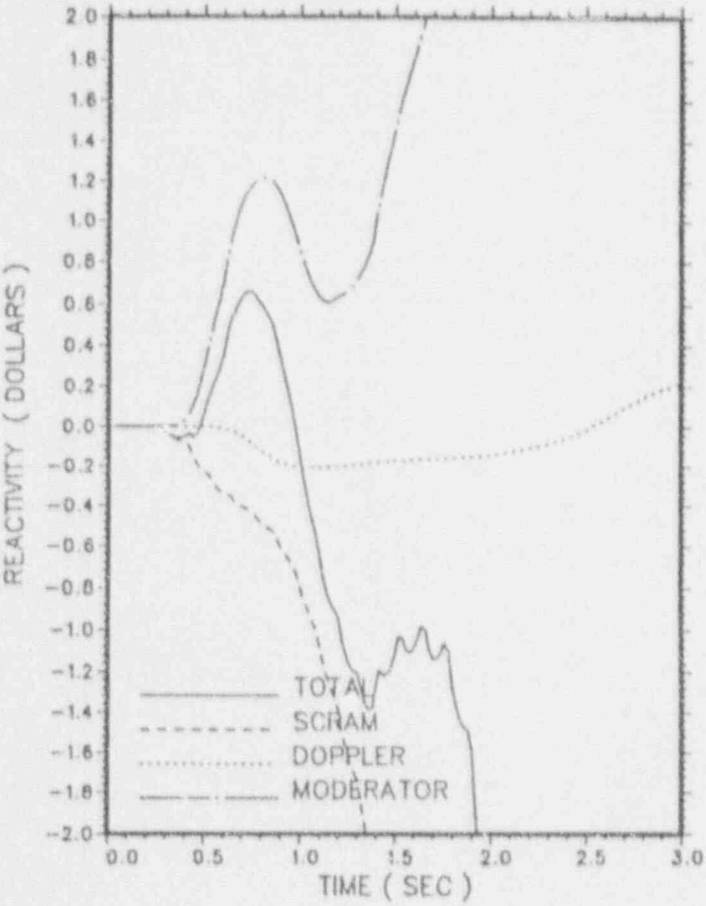

FIGURE 7.2.1
(Continued)

Turbine Trip Without Bypass, EOFPL16
Transient Response Versus Time, "Measured" S m Time

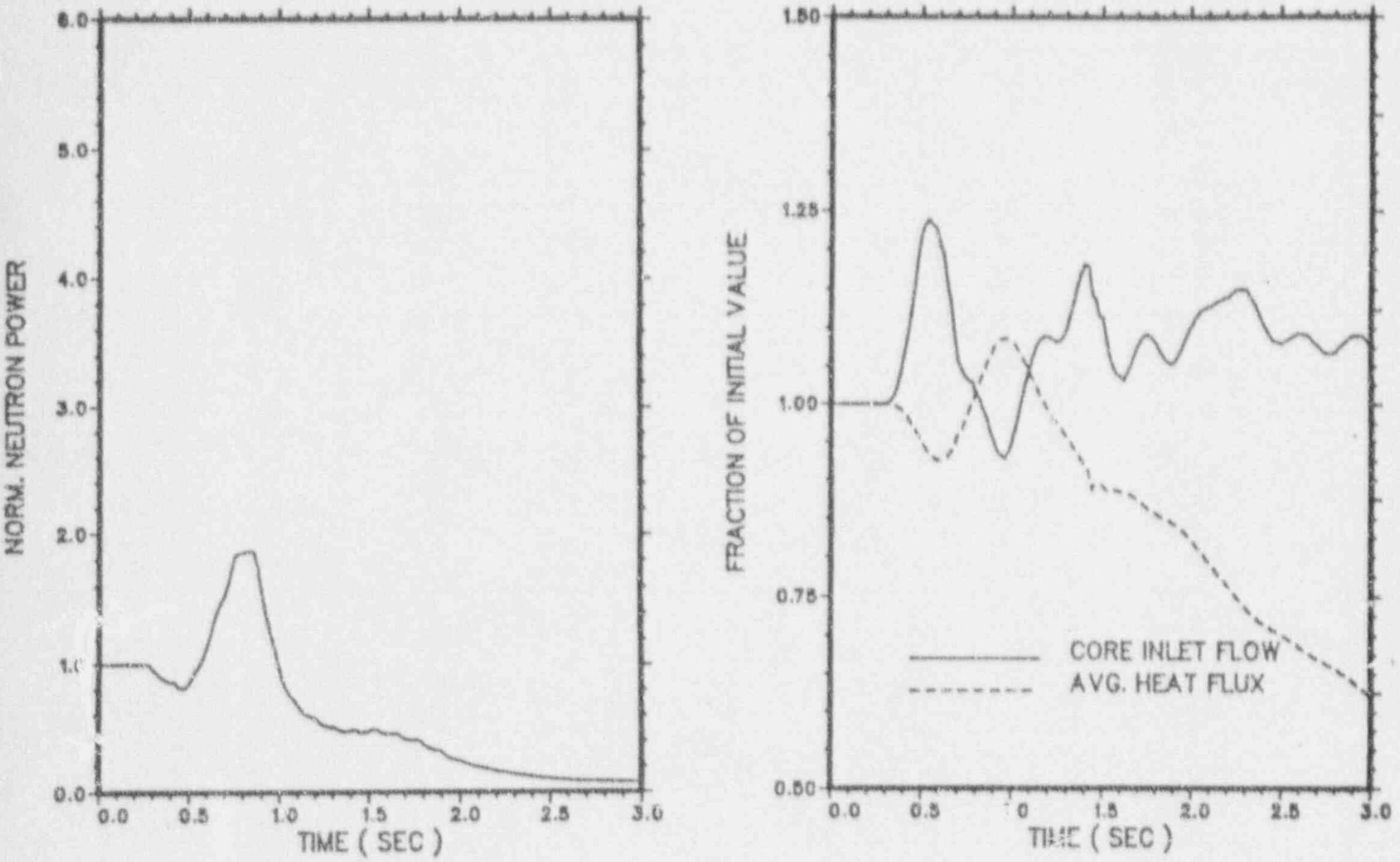

FIGURE 7.2.2

Turbine Trip Without Bypass, EOFPL16-1000 MWd/St
Transient Response Versus Time, "Measured" Scram Time

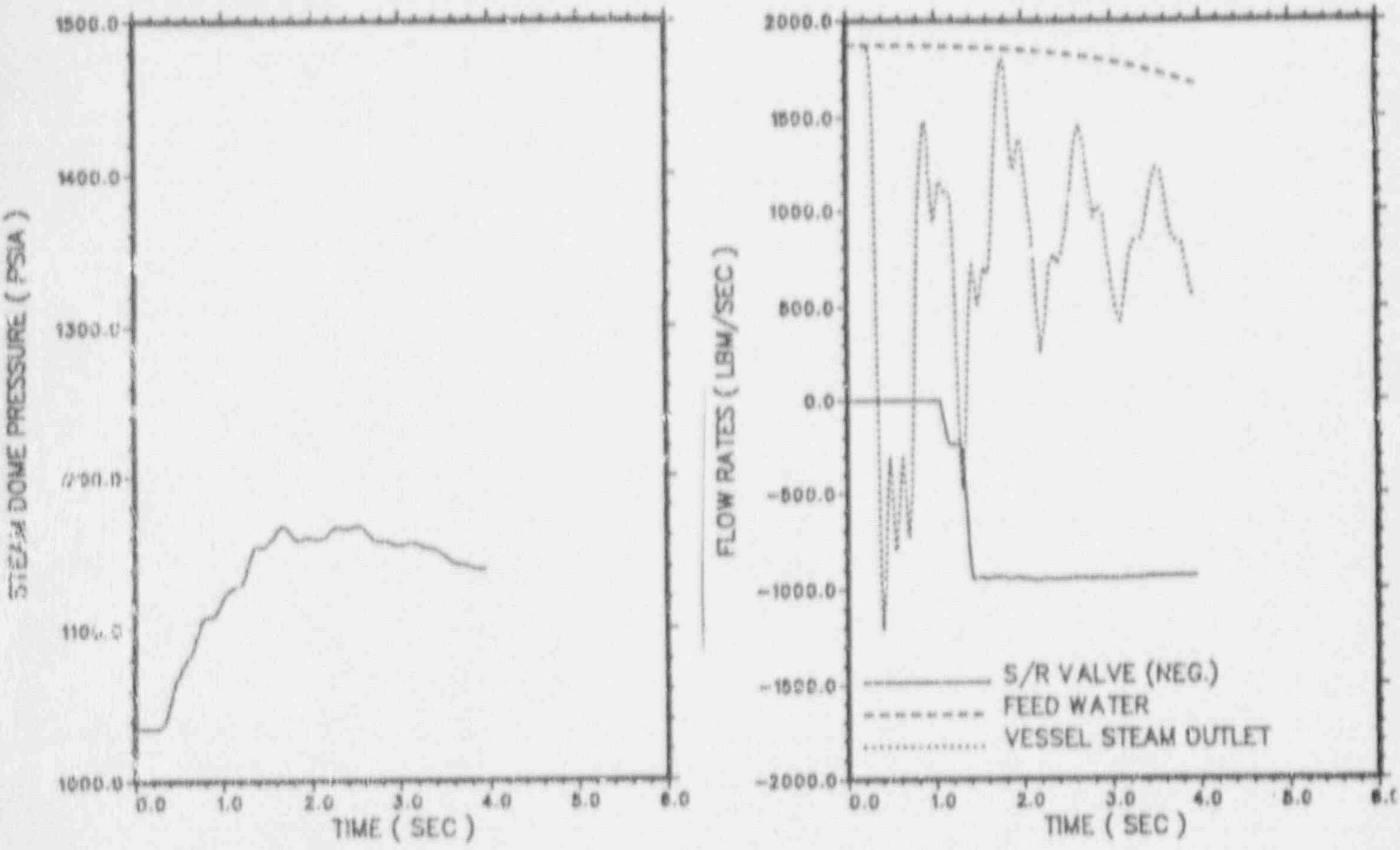

FIGURE 7.2.2
(Continued)

Turbine Trip Without Bypass, EOFPL16-1000 MWd/St
Transient Response Versus Time, "Measured" Scram Time

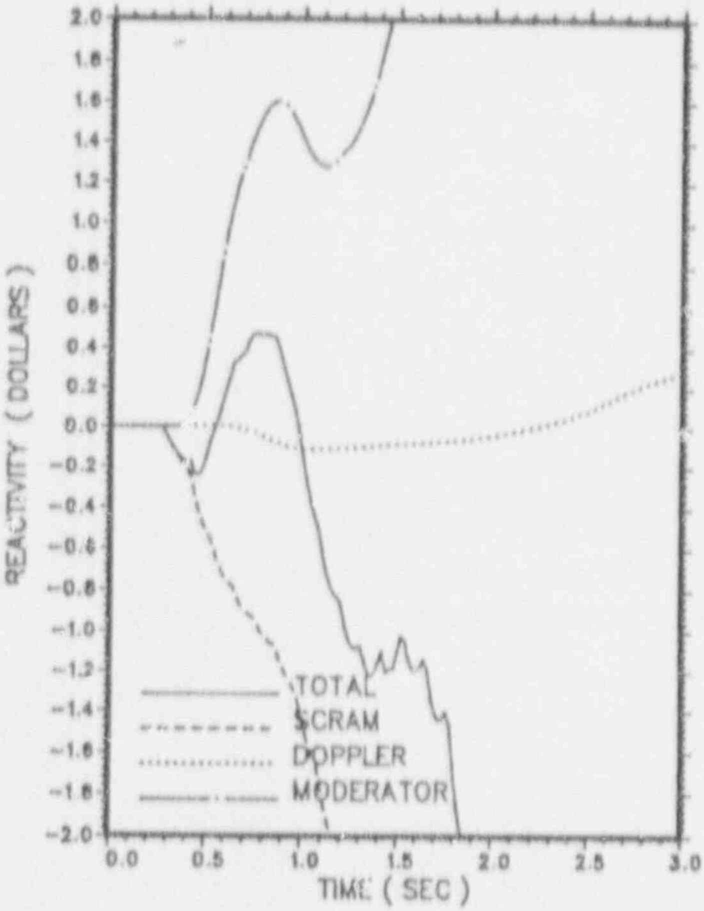

FIGURE 7.2.2
(Continued)

Turbine Trip Without Bypass, EOFPL16-1000 MWd/St
Transient Response Versus Time, "Measured" Scram Time

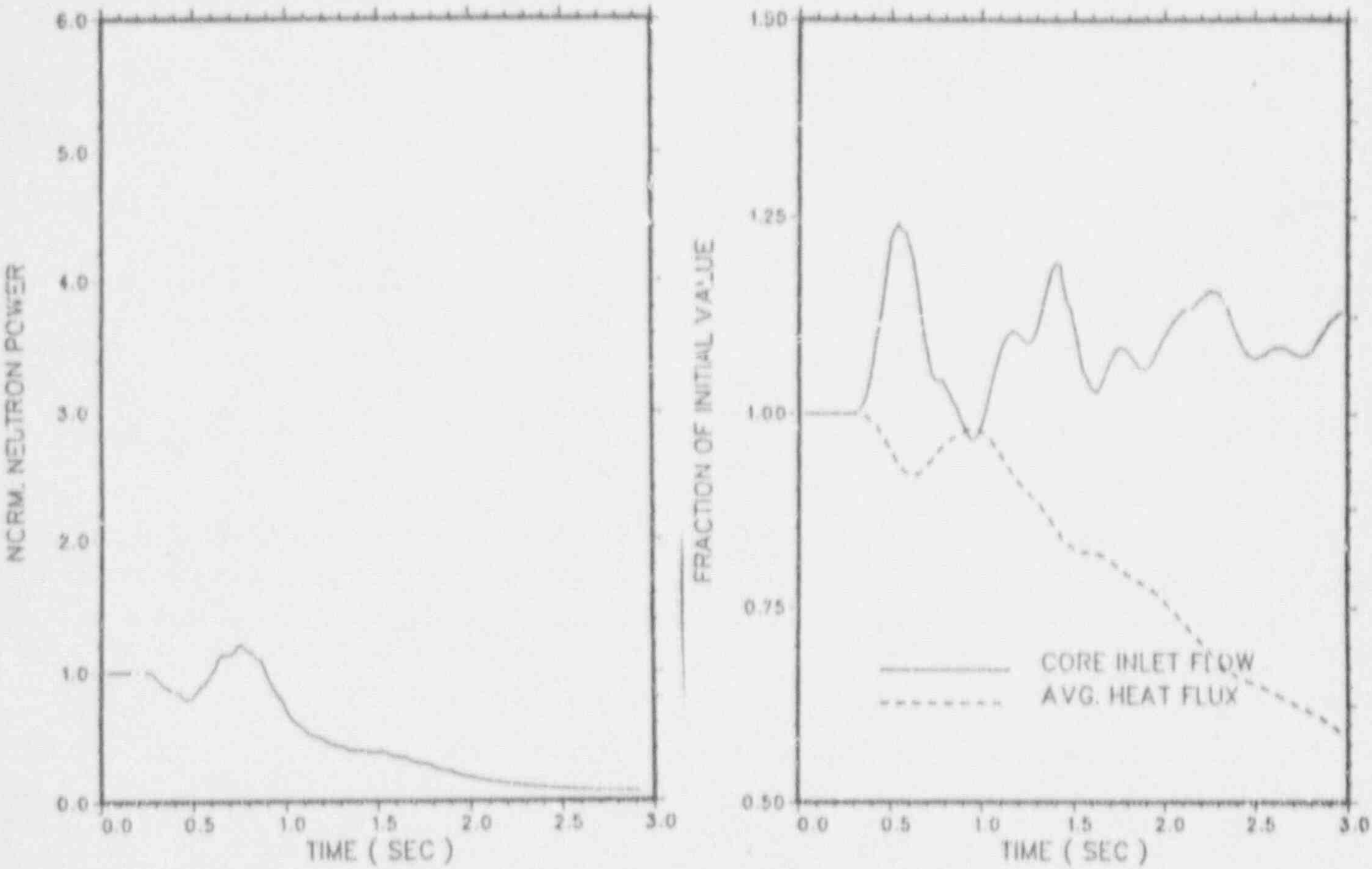

FIGURE 7.2.3

Turbine Trip Without Bypass, EOFPL-2000 MWd/St
Transient Response Versus Time, "Measured" Scram Time

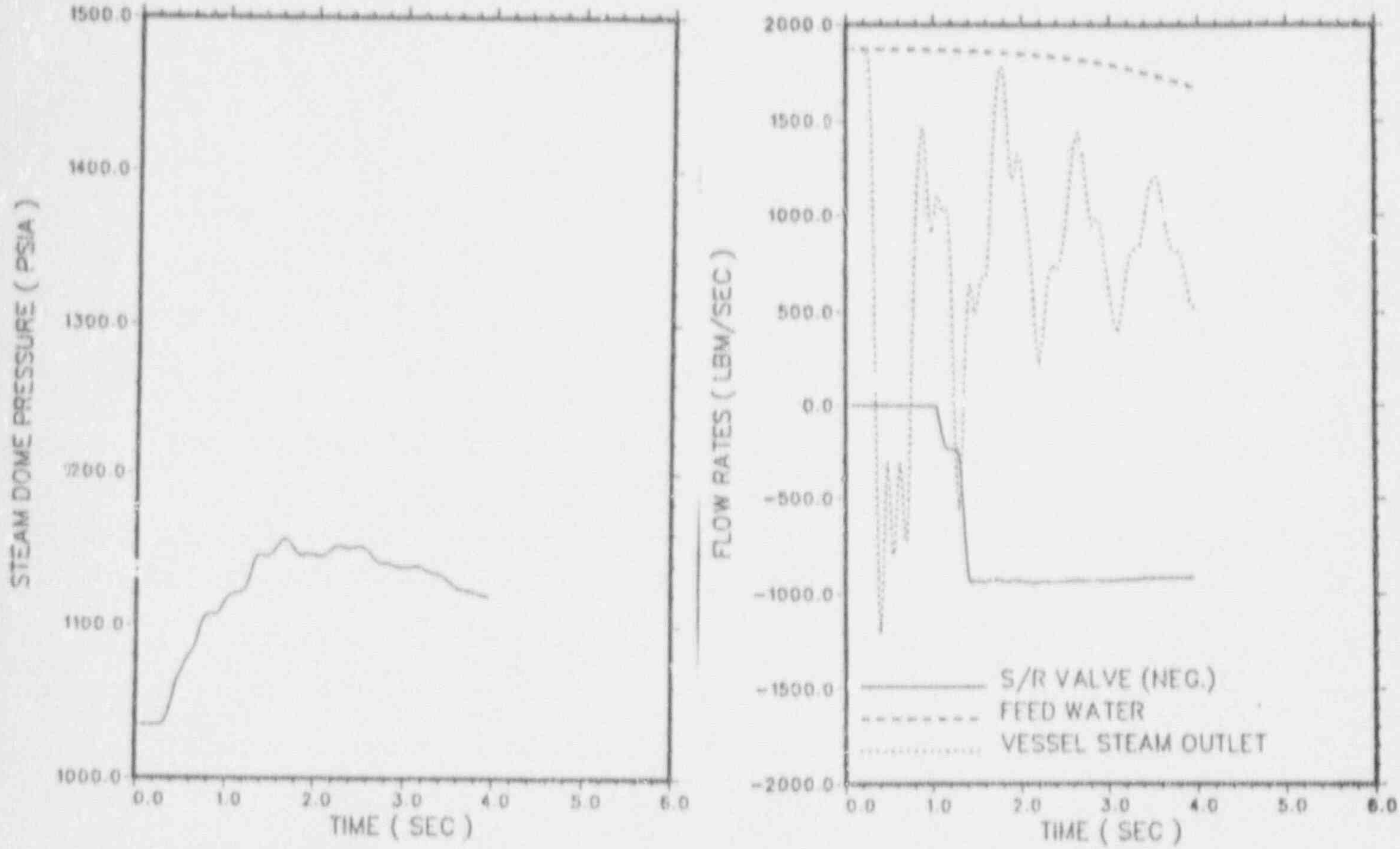

FIGURE 7.2.3
(Continued)

Turbine Trip Without Bypass, EOFPL-2000 MWd/St
Transient Response Versus Time, "Measured" Scram Time

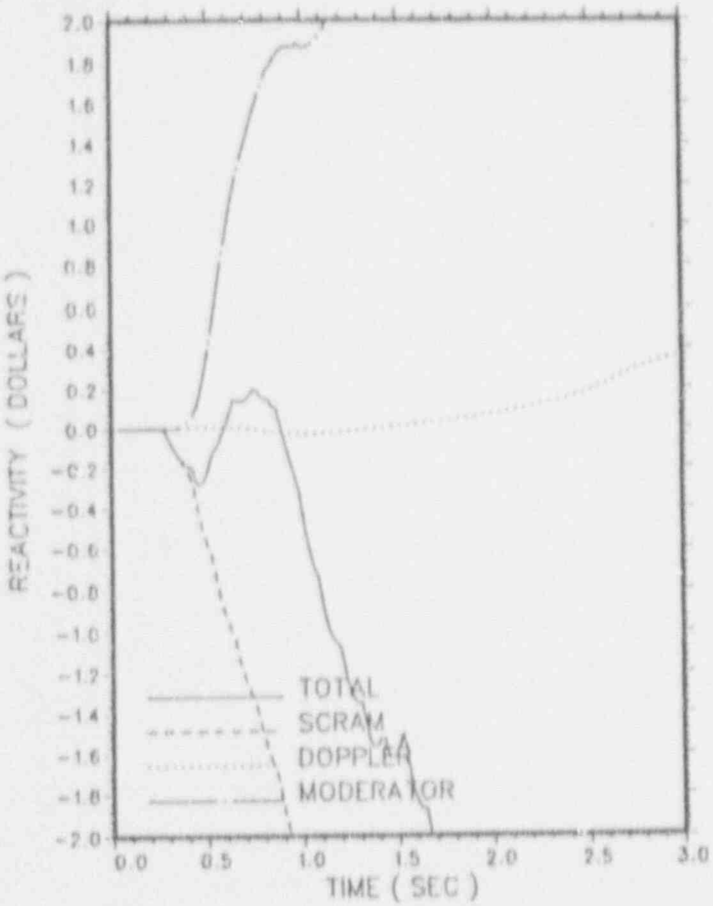

FIGURE 7.2.3
(Continued)

Turbine Trip Without Bypass, EOFPL-2000 MWd/St
Transient Response Versus Time, "Measured" Scram Time

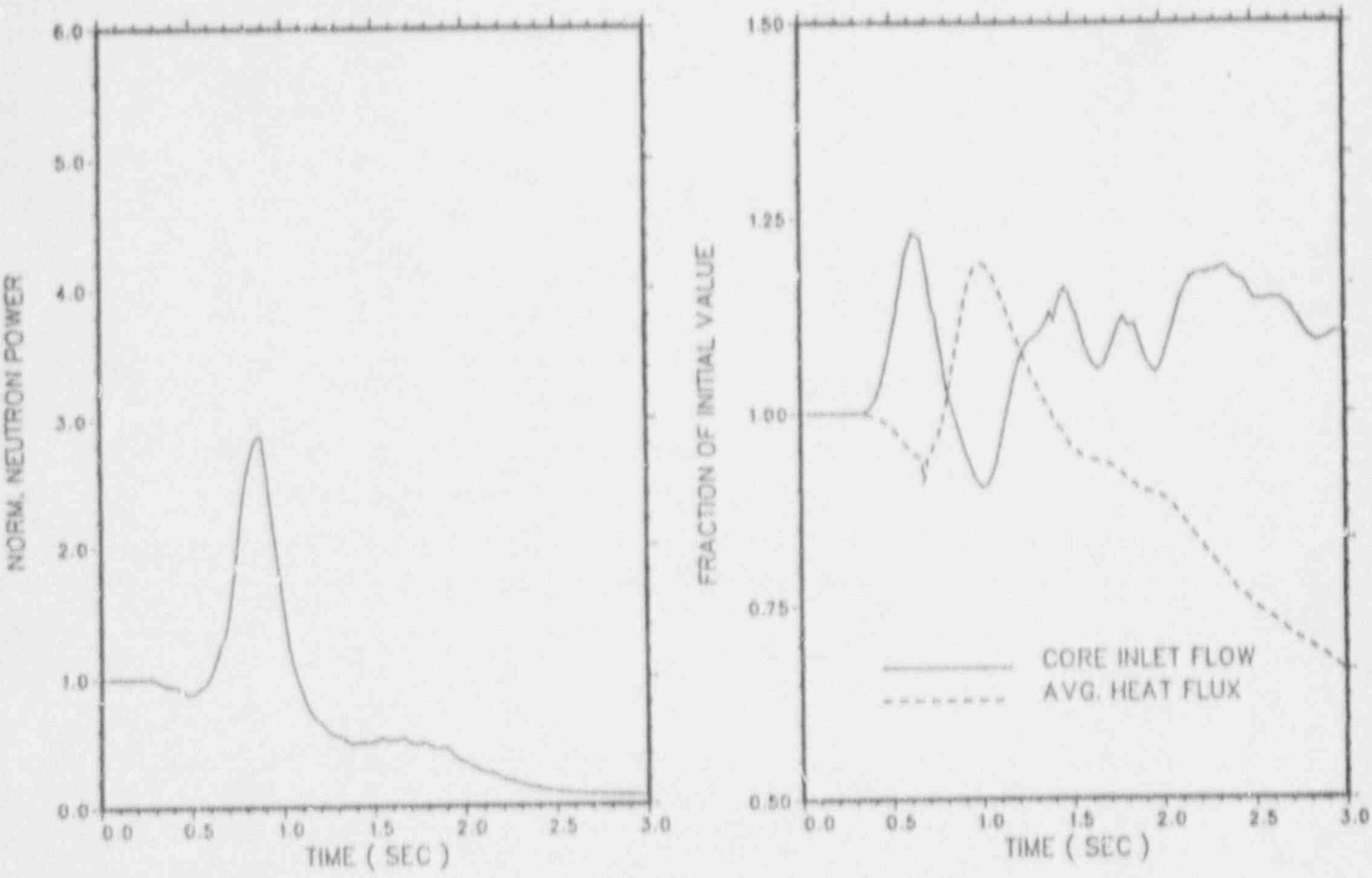

FIGURE 7.2.4

Generator Load Rejection Without Bypass, EOFPL16
Transient Response Versus Time, "Measured" Scram Time

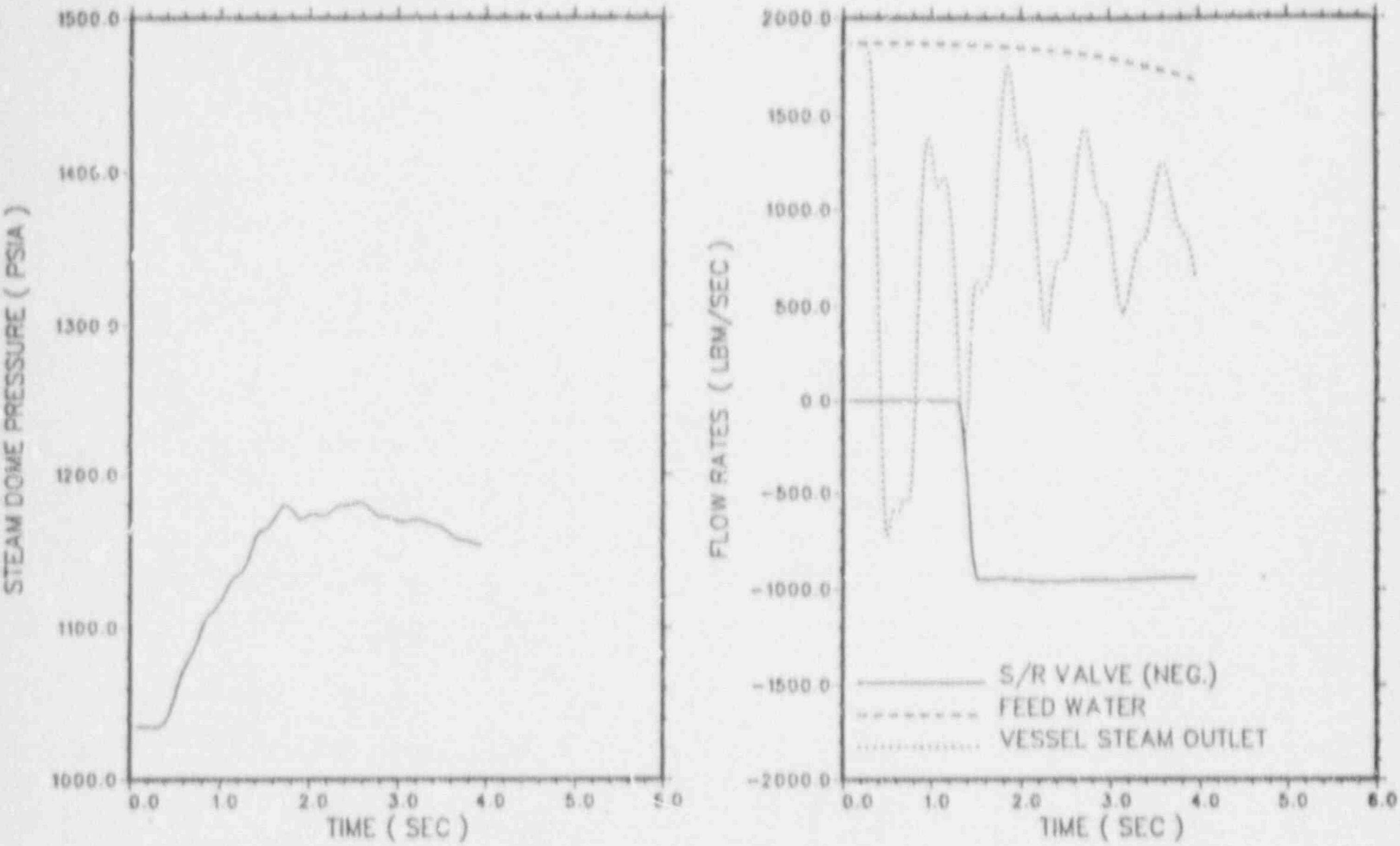

FIGURE 7.2.4
(Continued)

Generator Load Rejection Without Bypass, EOFPL16
Transient Response Versus Time, "Measured" Scram Time

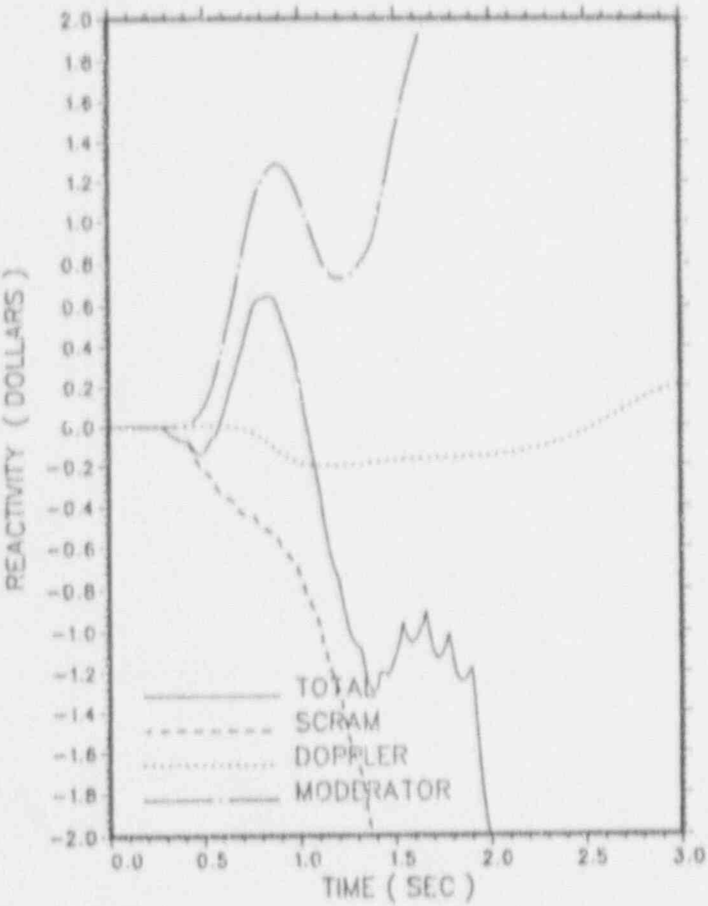

FIGURE 7.2.4
(Continued)

Generator Load Rejection Without Bypass, EOFPL16
Transient Response Versus Time, "Measured" Scram Time

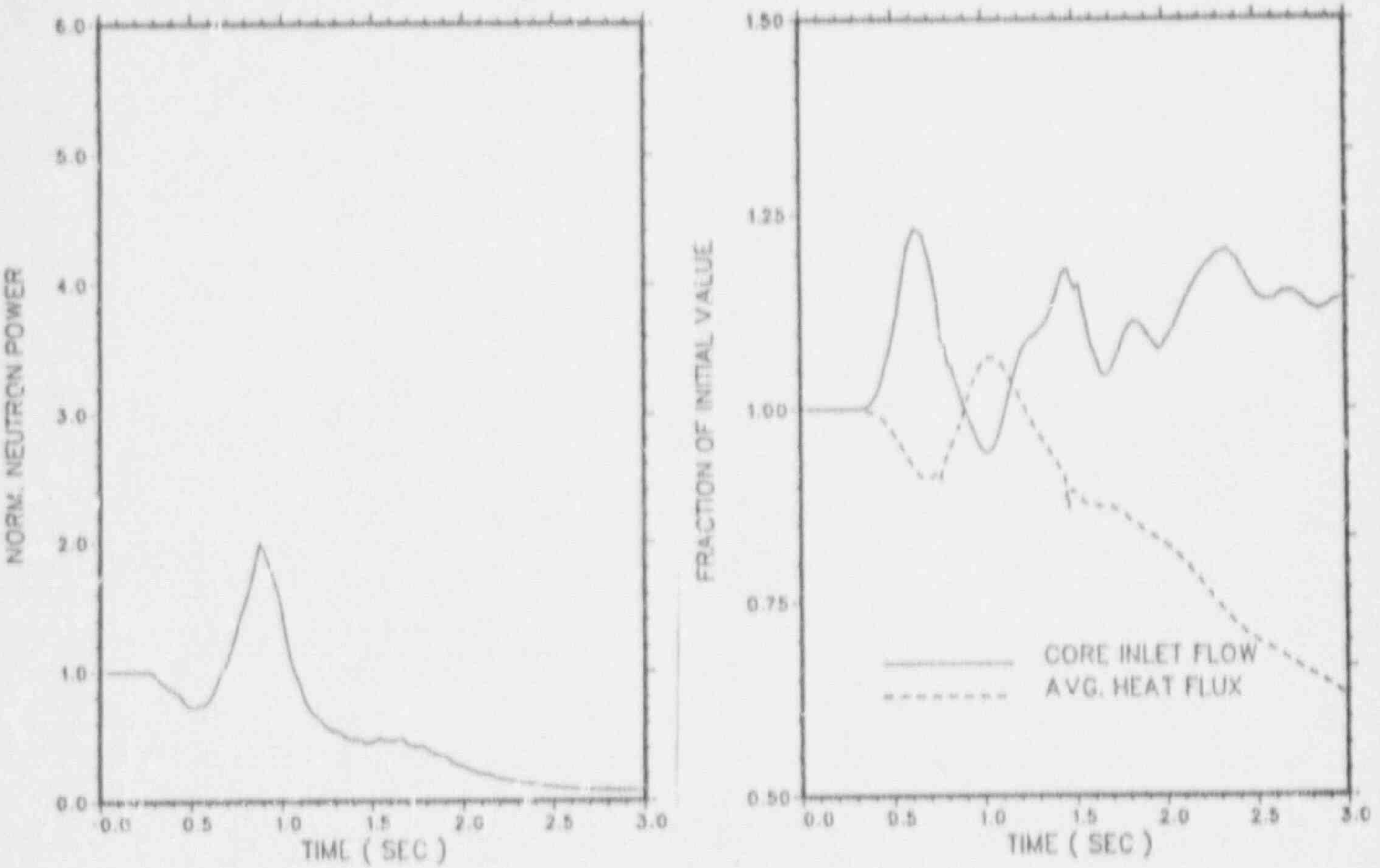

FIGURE 7.2.5

Generator Load Rejection Without Bypass, EOFPL16-1000 MWd/St
Transient Response Versus Time, "Measured" Scram Time

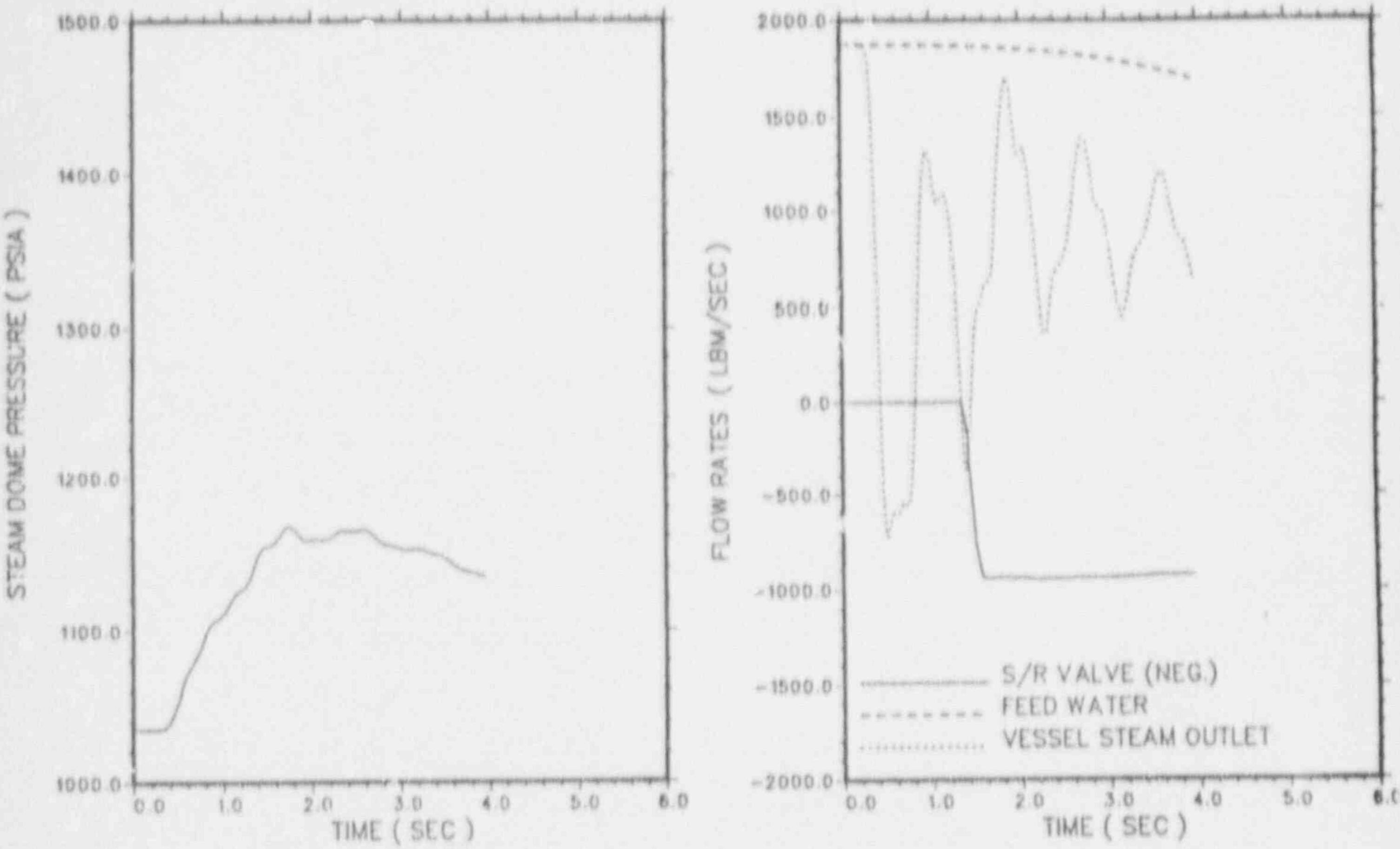

FIGURE 7.2.5
(Continued)

Generator Load Rejection Without Bypass, EOFPL16-1000 MWd/St
Transient Response Versus Time, "Measured" Scram Time

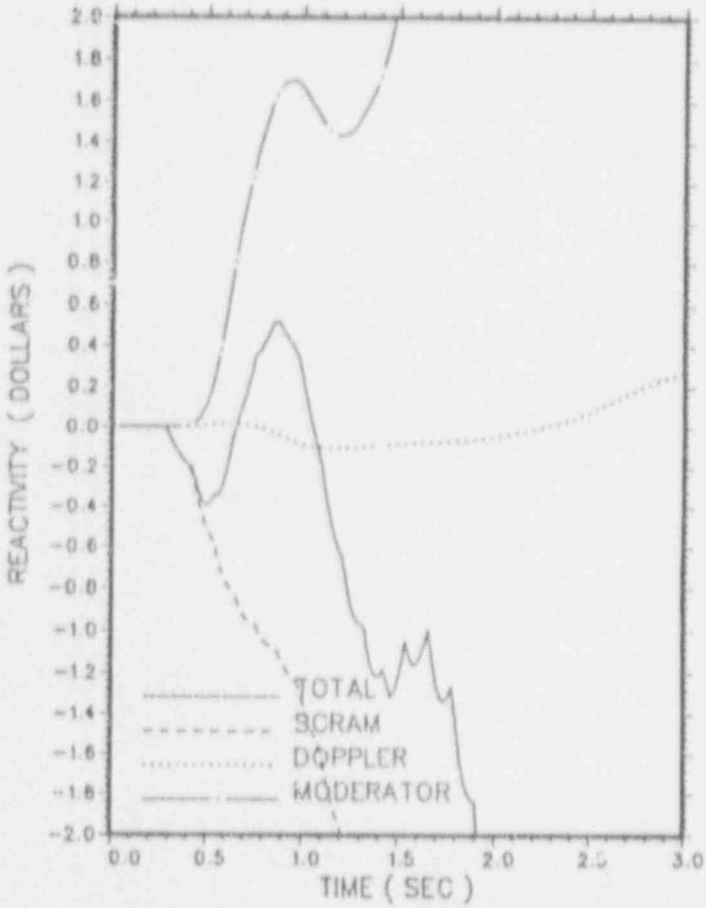

FIGURE 7.2.5
(Continued)

Generator Load Rejection Without Bypass, EOFPL16-1000 MWd/St
Transient Response Versus Time, "Measured" Scram Time

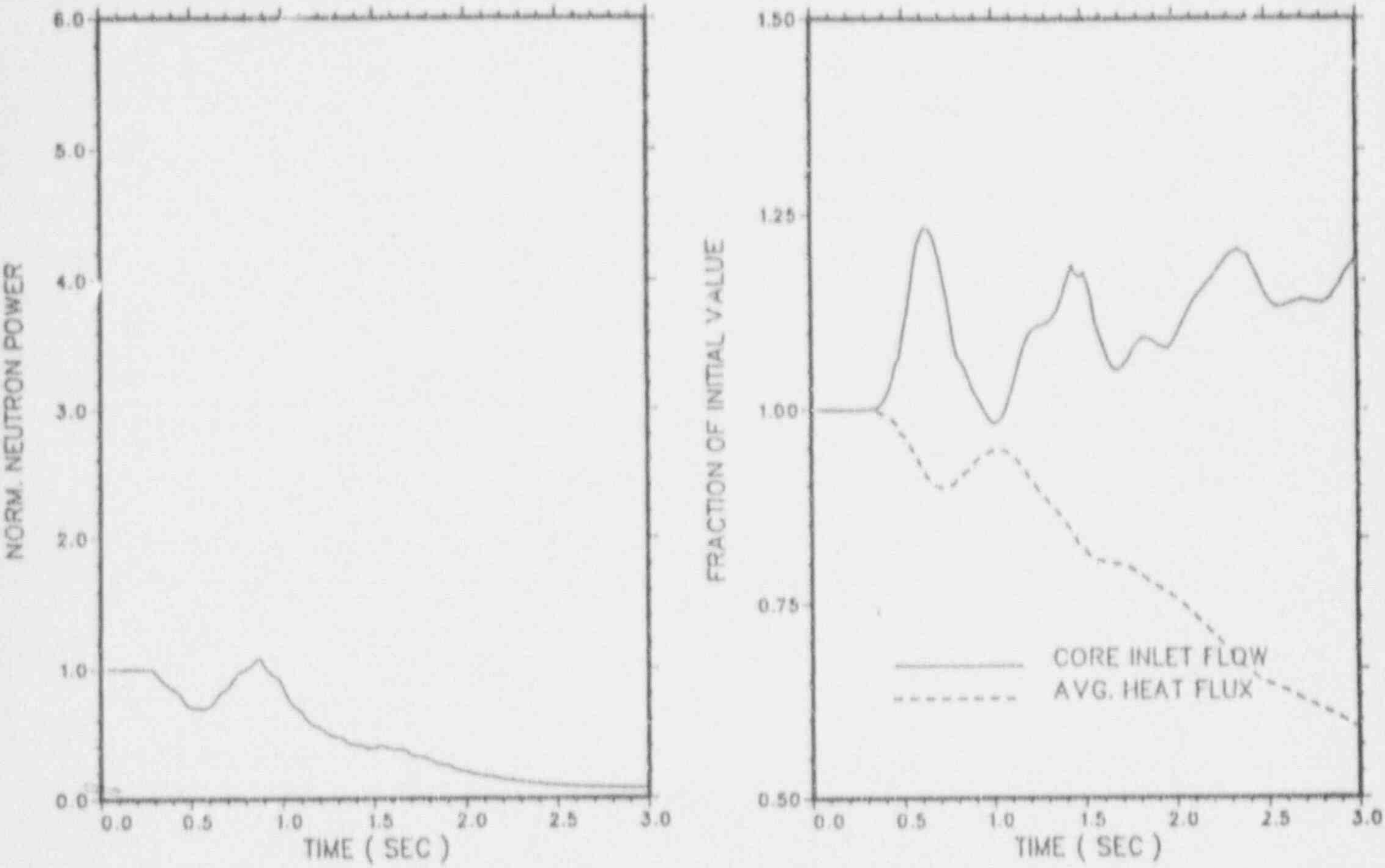

FIGURE 7.2.6

Generator Load Rejection Without Bypass, EOFPL16-2000 MWd/St
Transient Response Versus Time, "Measured" Scram Time

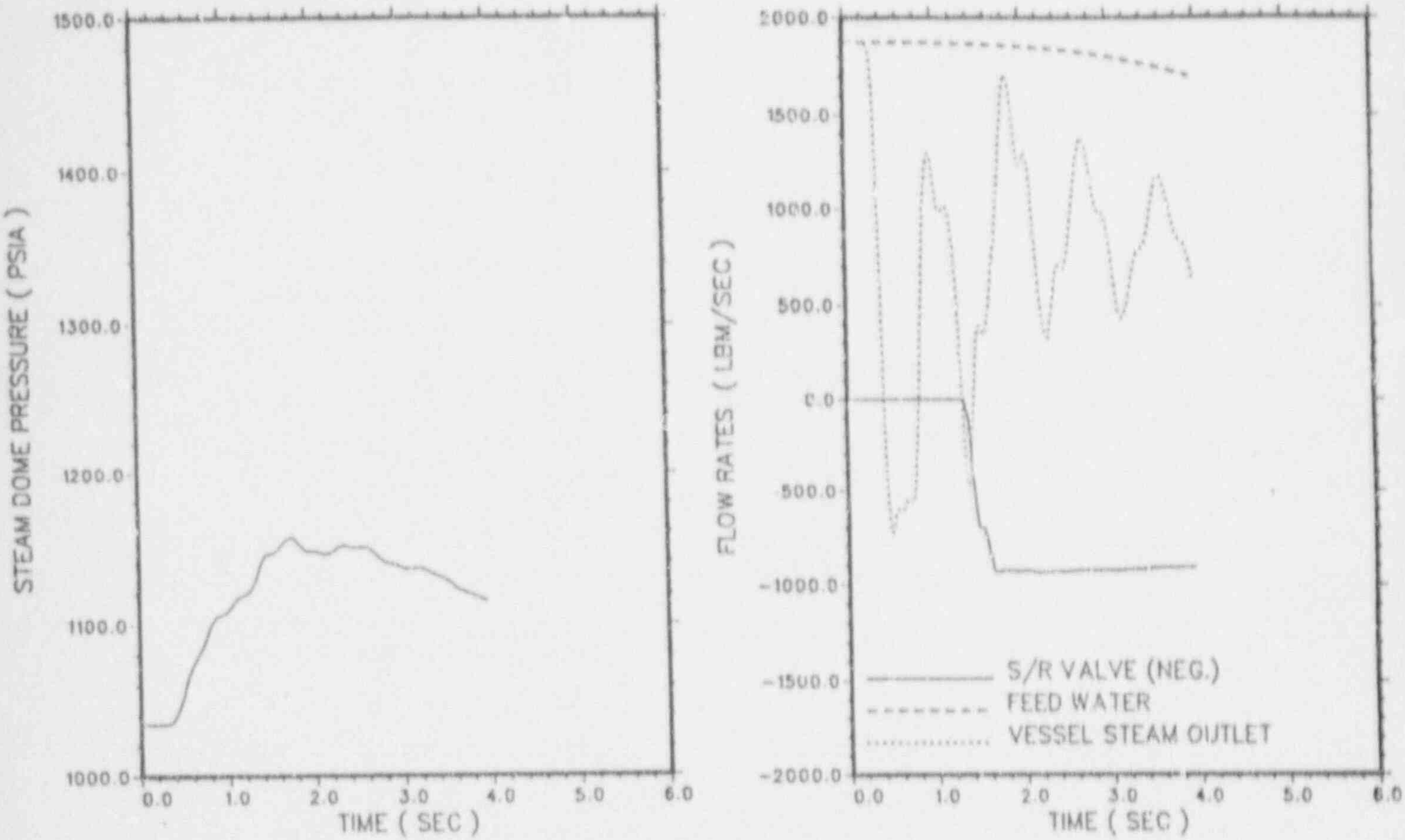

<u>FIGURE 7.2.6</u>
(Continued)

<u>Generator Load Rejection Without Bypass, EOFPL16-2000 MWd/St</u>
<u>Transient Response Versus Time, "Measured" Scram Time</u>

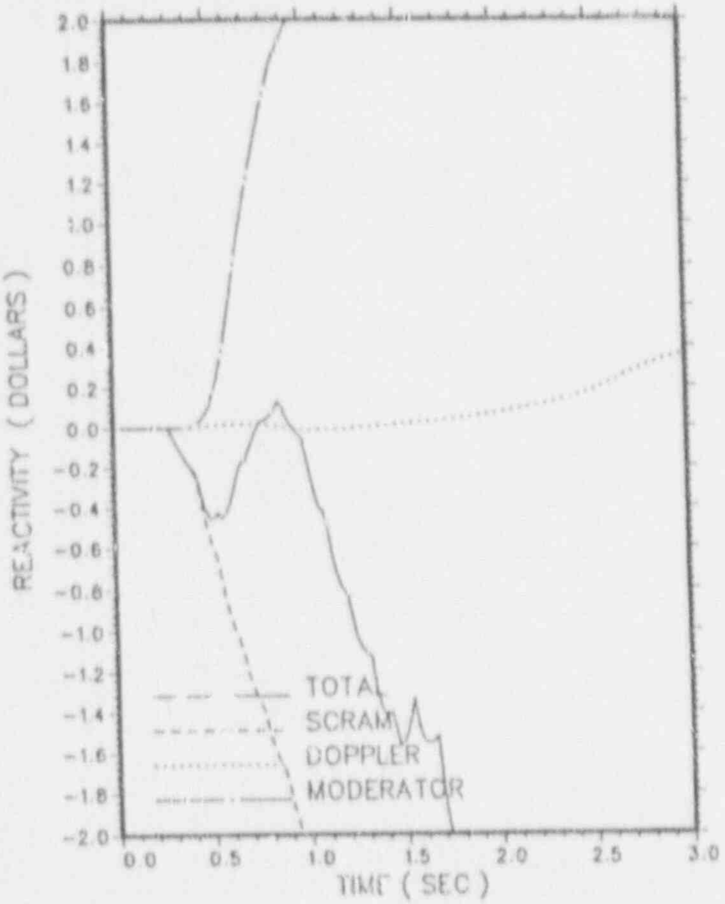

FIGURE 7.2.6
(Continued)

Generator Load Rejection Without Bypass, EOFPL16-2000 MWd/St
Transient Response Versus Time, "Measured" Scram Time

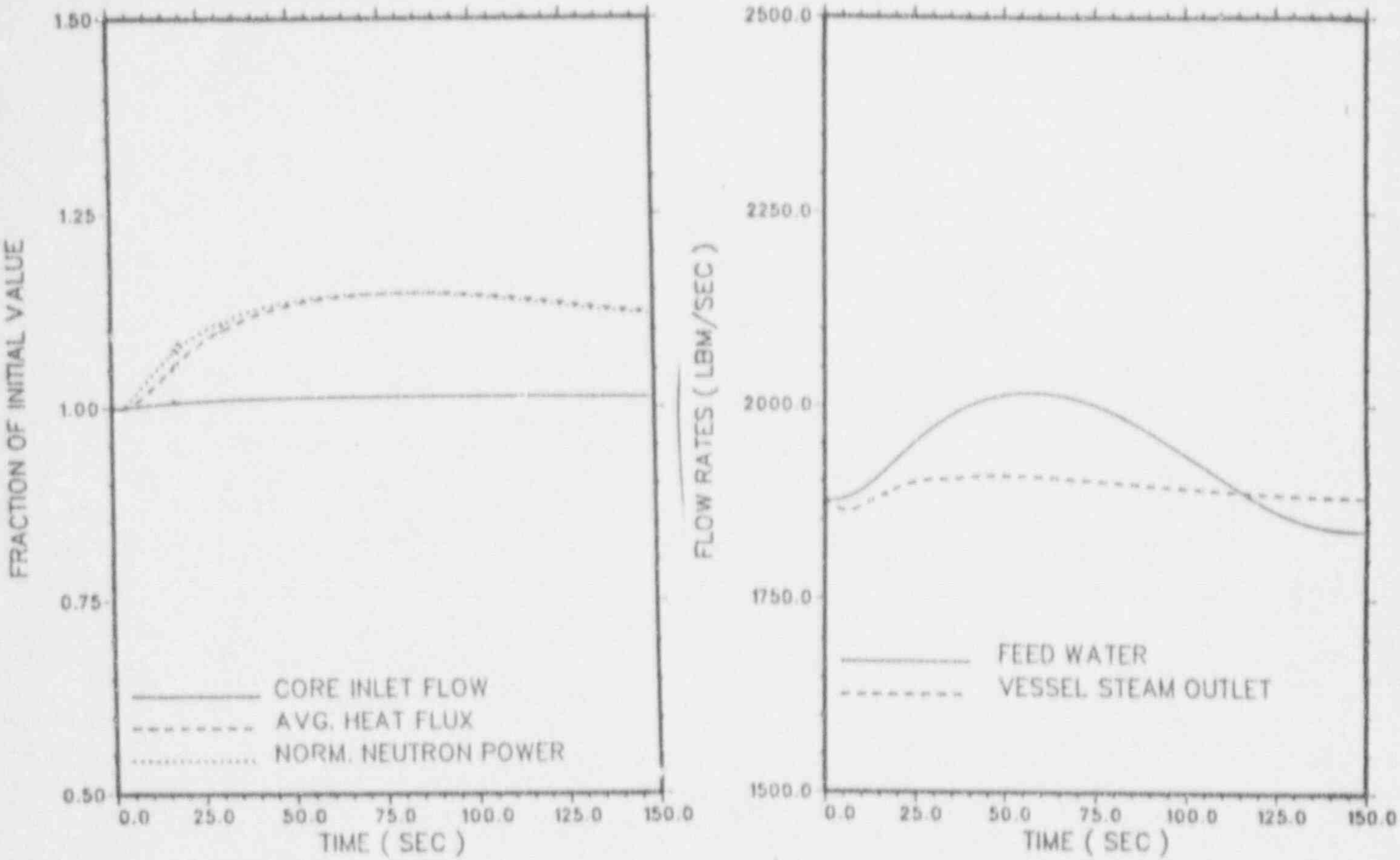

FIGURE 7.2.7

Loss of 100°F Feedwater Heating, BOC16 (Limiting Case)
Transient Response Versus Time

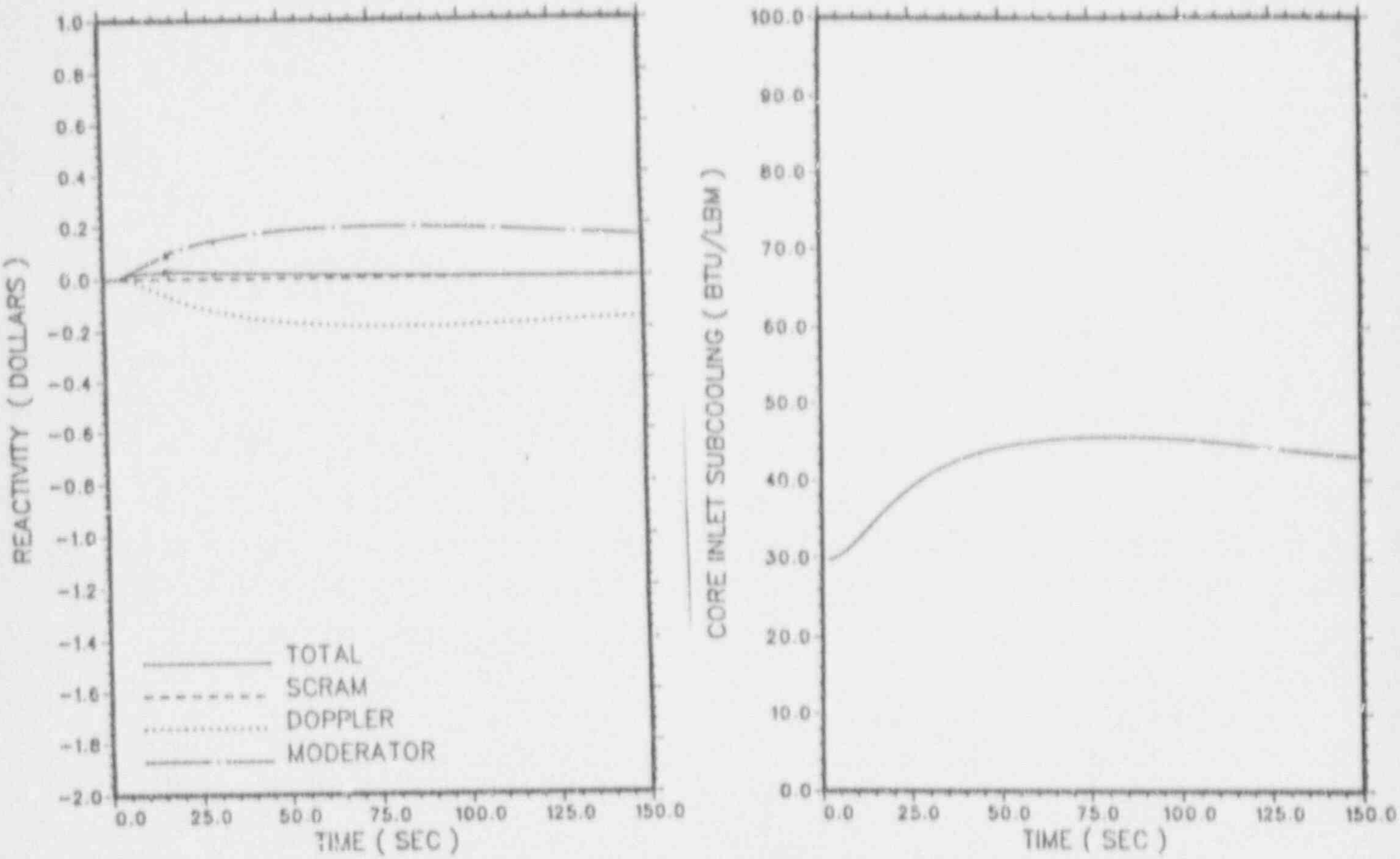

FIGURE 7.2.7
(Continued)

Loss of 100°F Feedwater Heating, BOC16 (Limiting Case)
Transient Response Versus Time

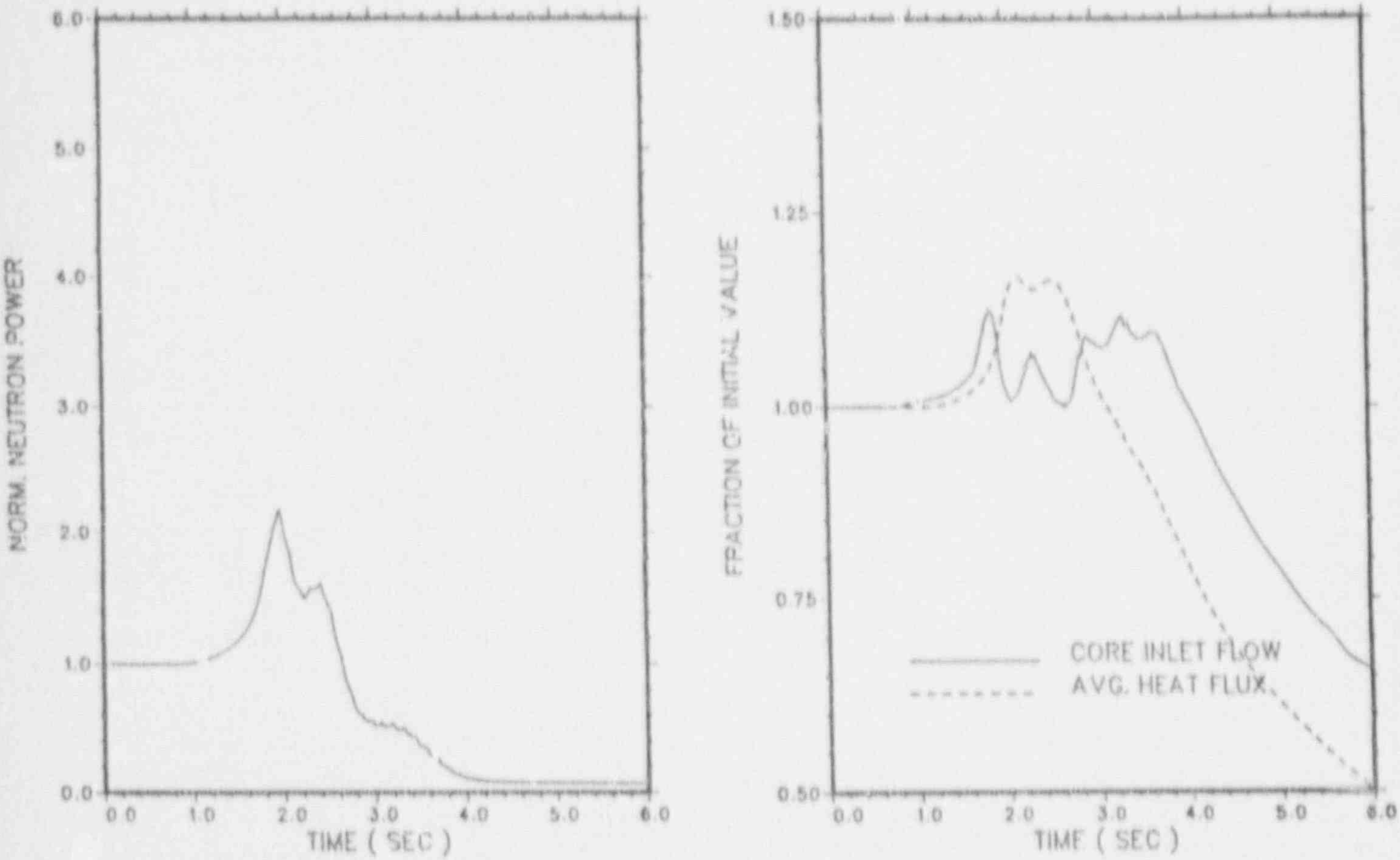

FIGURE 7.3.1

MSIV Closure, Flux Scram, EOFPL16
Transient Response Versus Time, "Measured" Scram Time

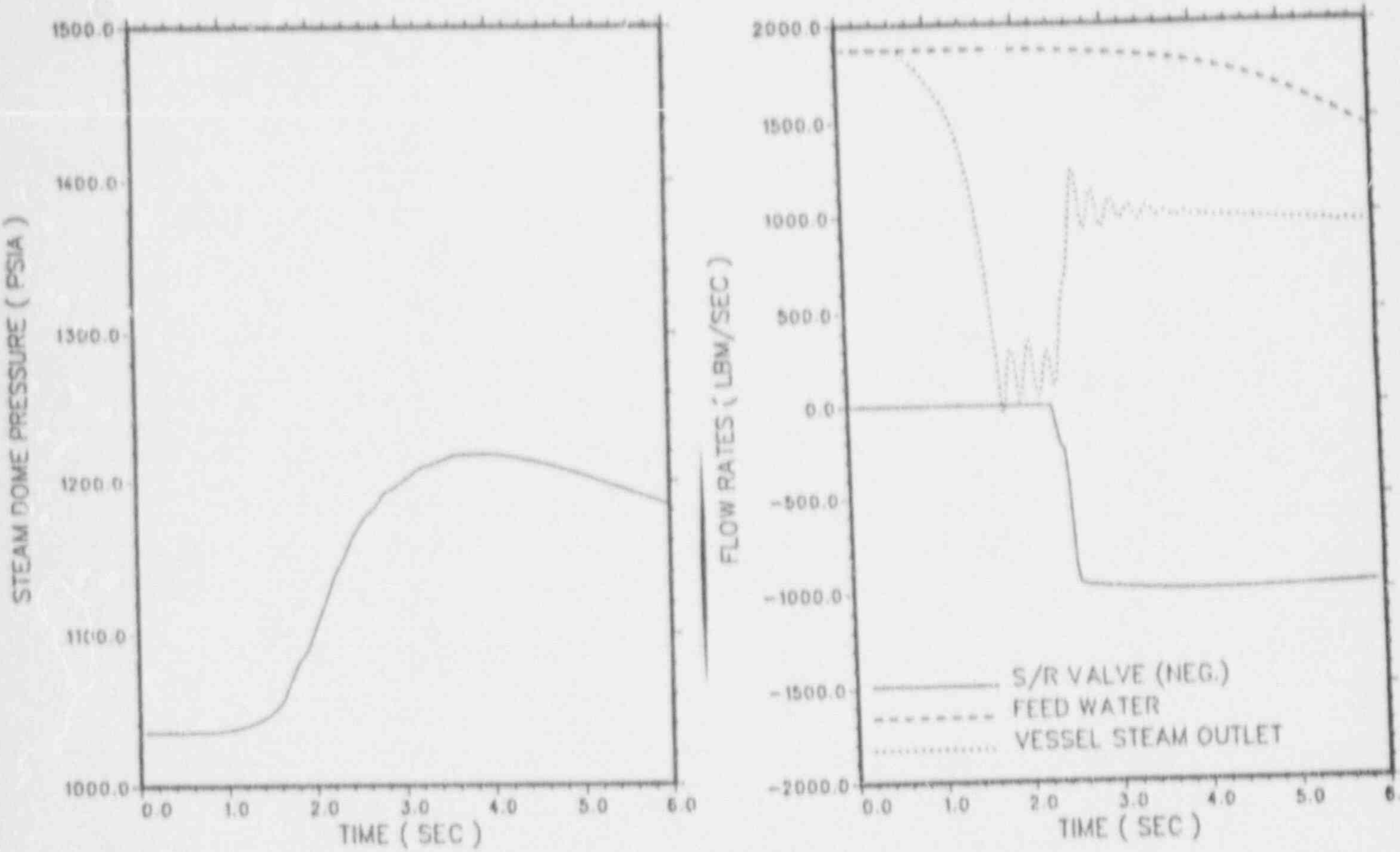

FIGURE 7.3.1
(Continued)

MSIV Closure, Flux Scram, EOFPL16
Transient Response Versus Time, "Measured" Scram Time

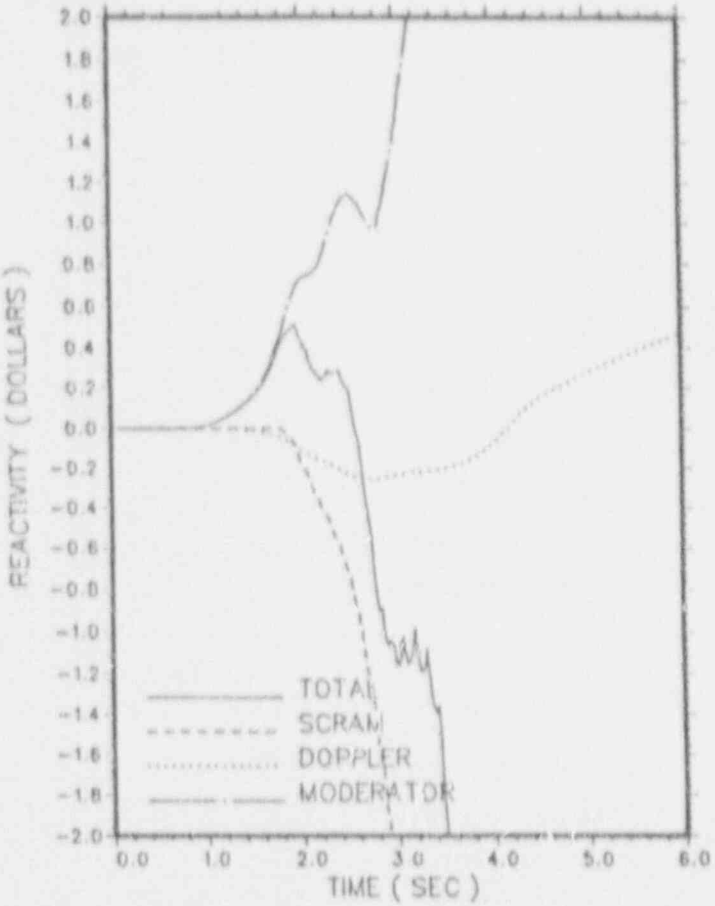

FIGURE 7.3.1
(Continued)

MSIV Closure, Flux Scram, EOFPL16
Transient Response Versus Time, "Measured" Scram Time

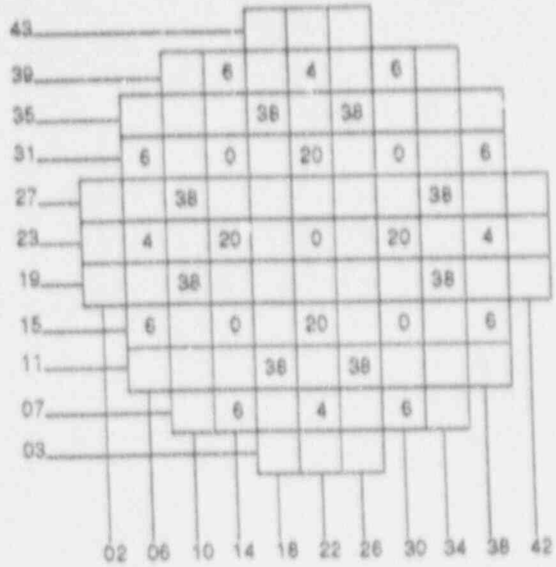

Core Thermal Power = 1664 MWt
Core Flow = 48 Mlb/hr
Core Exit Pressure = 1042 psia
Zero Xenon

Initial MCPR = 1.243
Initial MLHGR = 14.40 kw/ft
RWE Control Rod = 30-15

TRANSIENT SUMMARY

RBM Setpoint	Rod Position	ΔCPR	MLHGR (kw/ft)
104	10	0.12	15.1
105	12	0.16	15.4
106	12	0.16	15.4
107	14	0.21	16.6
108	16	0.25	17.8

FIGURE 7.4.1

Reactor Initial Conditions and Transient Summary for the VY Cycle 16 Rod Withdrawal Error Case 1

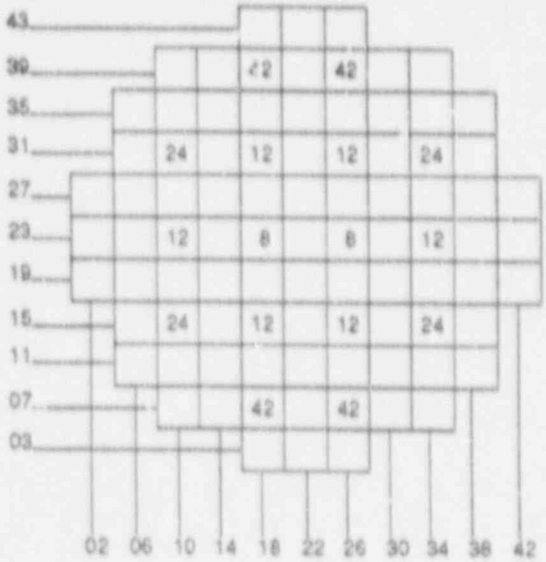

Core Thermal Power = 1664 MWt
Core Flow = 48 Mlb/hr
Core Exit Pressure = 1042 psia
Equilibrium Xenon

Initial MCPR = 1.530
Initial MLHGR = 11.5 kw/ft
RWE Control Rod = 26-23

TRANSIENT SUMMARY

RBM Setpoint	Rod Position	ΔCPR	MLHGR. (kw/ft)
104	18	0.10	14.8
105	20	0.11	15.0
106	20	0.11	15.0
107	24	0.14	15.3
108	34	0.18	14.7

FIGURE 7.4.2

Reactor Initial Conditions and Transient Summary for the VY Cycle 16 Rod Withdrawal Error Case 2

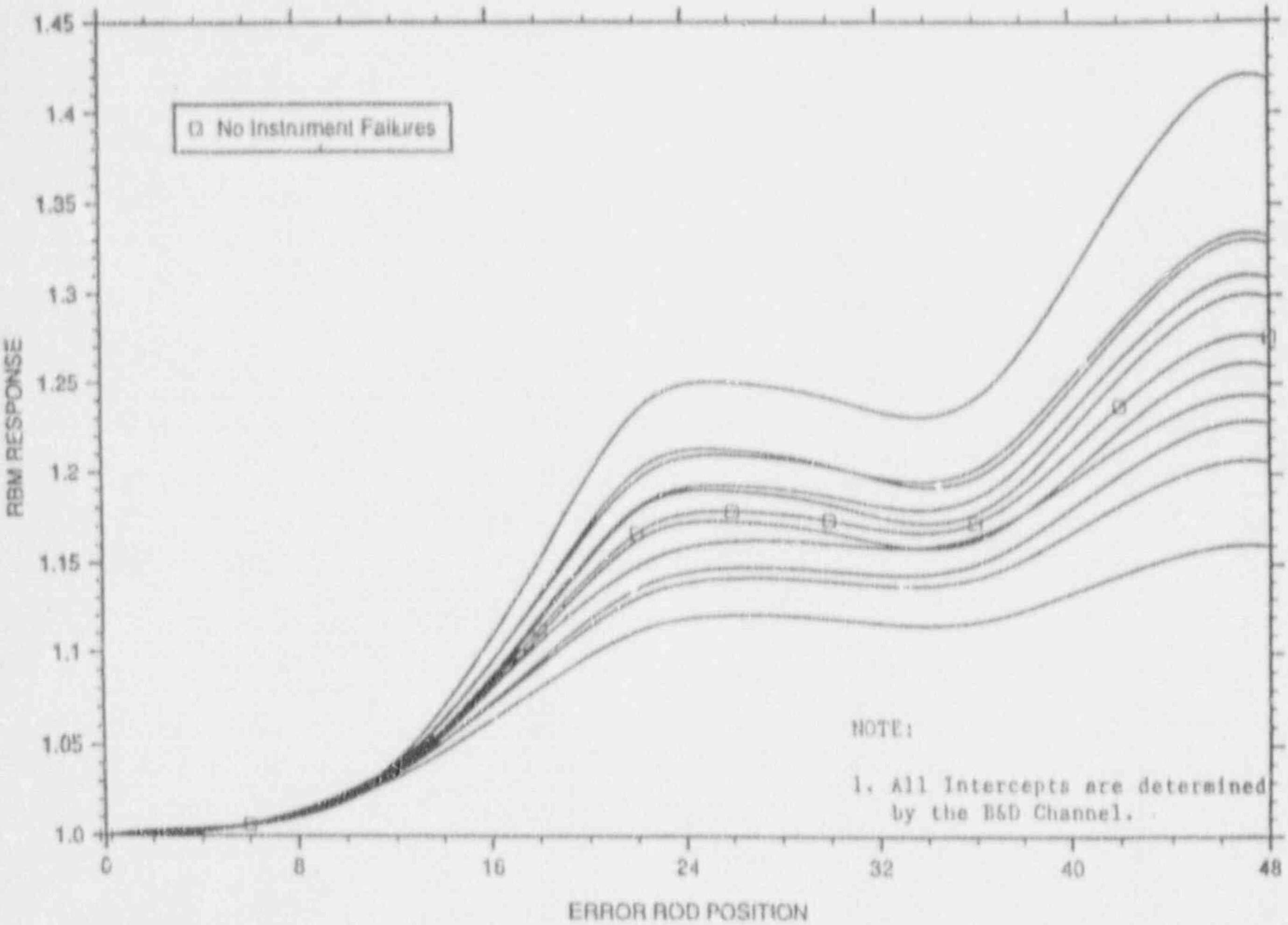

FIGURE 7.4.3

VY Cycle 16 RWE Case 1 - Setpoint Intercepts Determined by the A and C Channels

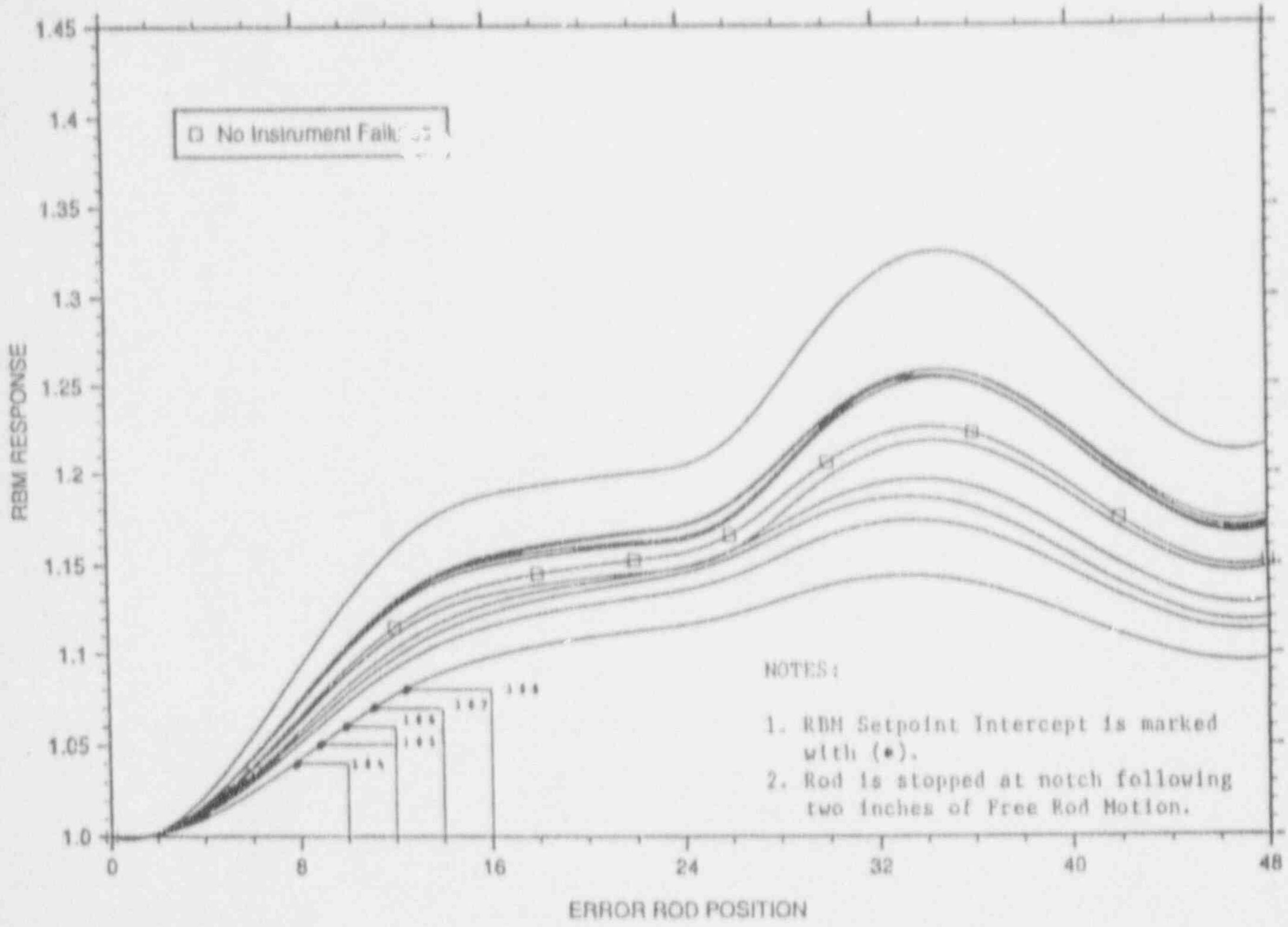

FIGURE 7.4.4

VY Cycle 16 RWE Case 1 - Setpoint Intercepts Determined by the B and D Channels

8.0 DESIGN BASIS ACCIDENT ANALYSIS

8.1 Control Rod Drop Accident Results

The control rod sequences are a series of rod withdrawal and banked withdrawal instructions specifically designed to minimize the worths of individual control rods. The sequences are examined so that, in the event of the uncoupling and subsequent free fall of the rod, the incremental rod worth is acceptable. Incremental rod worth refers to the fact that rods beyond Group 2 are banked out of the core and can only fall the increment from full-in to the rod drive withdrawal position. Acceptable worth is one which produces a maximum fuel enthalpy less than 280 calories/gram.

Some out-of-sequence control rods could accrue potentially high worths. However, the Rod Worth Minimizer (RWM) will prevent withdrawing an out-of-sequence rod, if accidentally selected. The RWM is functionally tested before each startup.

The sequence in the RWM will take the plant from All Rods In (ARI) to well above 20% core thermal power. Above 20% power even multiple operator errors will not create a potential rod drop situation above 280 calories per gram[21],[22],[23]. Below 20% power, however, the sequences must be examined for incremental rod worth. This is done throughout the cycle using the full core, xenon-free SIMULATE-3 model.

Both the A and B sequences were examined at various exposures throughout the cycle. For startup, the rods are grouped, as shown in Figures 8.1.1 and 8.1.2, and are pulled in numerical order. All the rods in one group are pulled out before the pulling of the next group begins. The rods in the first two groups are individually pulled from full-in to full-out. Beyond Group 2, the rods are banked out using procedures[24],[25] which reduce the rod incremental worths.

The potentially high worths that occur in the pulling of the Group 1 rods are ignored because the reactor is subcritical in Group 1. Therefore, if a rod drops from any configuration in the first group, its excess reactivity contribution to the Rod Drop Accident (RDA) is zero. Successive reloads of axially zoned fuel have extended this subcriticality situation to the second group as well.

The second group of rods was examined using the analysis procedure[26]. Relatively few control rod configurations were found to be critical. For conservatism, "critical" was defined as the SIMULATE-3 average cold critical K_{eff} minus 1% ΔK (reactivity anomaly criteria). The few potentially critical configurations in Group 2 contributed less excess reactivity to the RDA than subsequent configurations in Group 3.

Most pre-drop cases in Group 3 are critical. Therefore, the entire dropped rod worth contributes toward the RDA excess reactivity insertion. The method used to evaluate Group 3 involved pulling Groups 1 and 2 out and banking Group 3 to varying positions. The types of cases examined included:

1. Banked positions 04, 08, 12, and 48 (full-out).

2. Group 3 rods pulled out of sequence, creating high flux regions.

3. Xenon-free conditions, both cold moderator and "standby" (i.e., 1020 psia).

4. Group 3 rods dropping from 00 (full-in) to the appropriate banked position.

5. Stuck rods from previously pulled Group 1 or 2 dropping from 00 to 48.

The highest worth results, presented in Table 8.1.1, fit under the bounding analysis in References 21 through 23.

8.2 Loss-of-Coolant Accident Analysis

The results of the complete evaluation of the loss-of-coolant accident for Vermont Yankee[27] provide the required support for the operation of the Reload Cycle. The LOCA analysis performed in accordance with 10CFR50, Appendix K, demonstrates that the MAPLHGR values comply with the ECCS limits specified in 10CFR50.46. The MAPLHGR limits for all the fuel types in the Reload Cycle, as a function of average planar exposure, are provided in Appendix A. Only the limiting MAPLHGR limits for the zoned fuel are provided in Appendix A. MAPLHGR limits exist for each lattice type and are specified in the process computer.

8.3 Refueling Accident Results

If any assembly is damaged during refueling, then a fraction of the fission product inventory could be released to the environment. The source term for the refueling accident is the maximum gap activity within any bundle. The source term includes contributions from both noble gases and iodines. The calculation of maximum gap activity is based on the MAPLHGRs, the maximum operating fuel centerline temperatures, and maximum bundle burnup.

The fuel rod gap activity for the Reload Cycle is bounded by the values used in Section 14.9 of the FSAR[28].

TABLE 8.1.1

VY Cycle 16 Control Rod Drop Analysis Results

Maximum Incremental Rod Worth Calculated Cold, Xenon-Free	0.61% ΔK
Bounding Analysis Worth for Enthalpy Less than 280 Calories per Gram [21],[22],[23]	1.30% ΔK

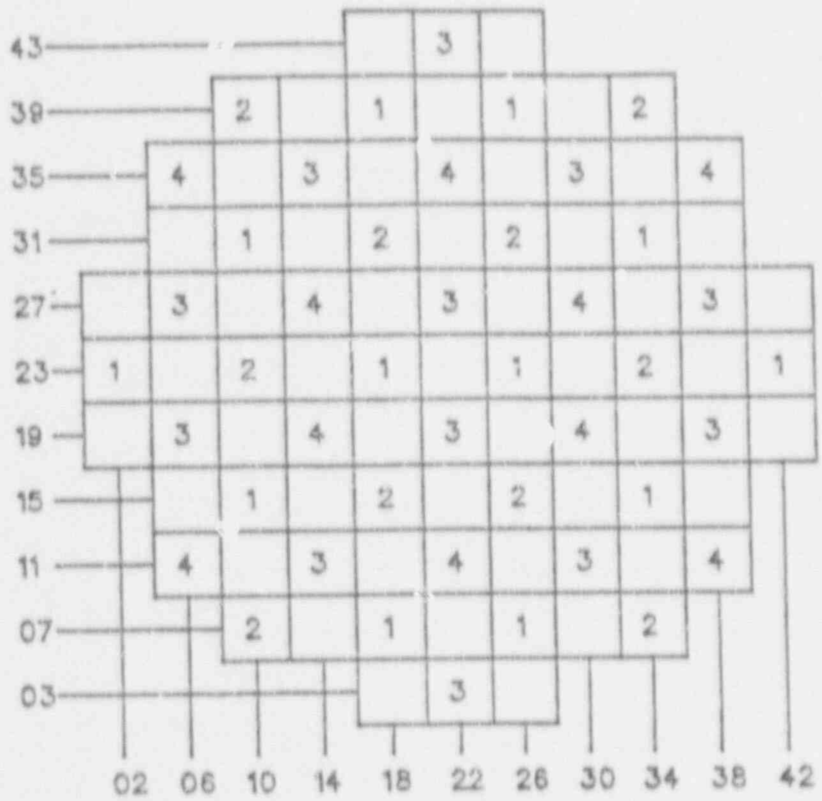

FIGURE 8.1.1

First Four Rod Arrays Pulled in the A Sequences

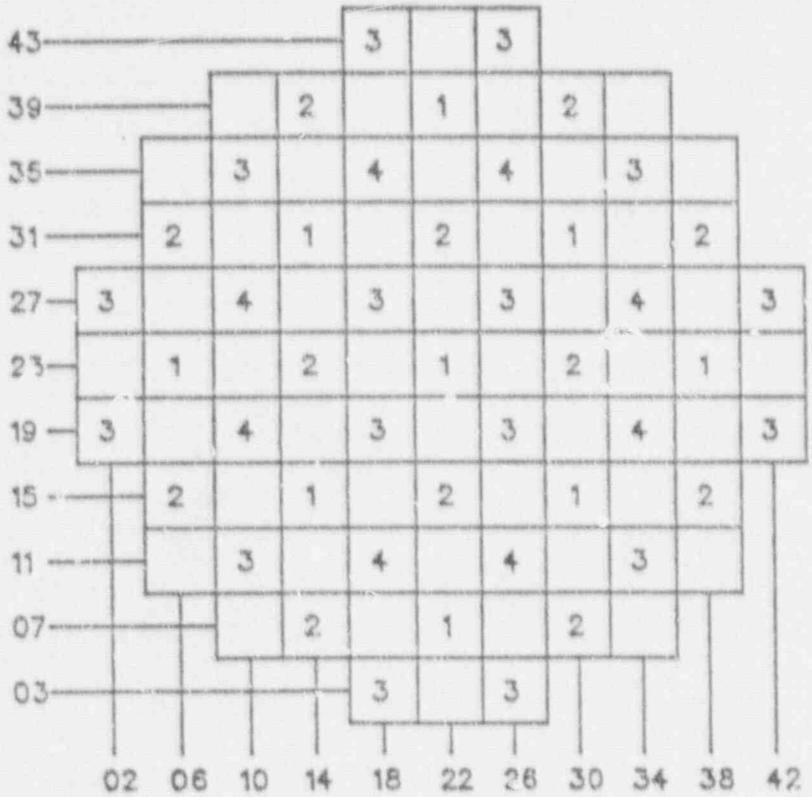

FIGURE 8.1.2

First Four Rod Arrays Pulled in the B Sequences

9.0 CORE COMPONENT QUALIFICATION PROGRAM

9.1 Siemens Nuclear Power Fuel Assemblies

Vermont Yankee has four ANF-IX-3.04B-EGZ Qualification Fuel Assemblies (QFAs)[29] to qualify this bundle type for use as a potential reload bundle. The bundles were loaded into Cycle 15 and have been irradiated for one cycle. The ANF-IX QFAs were manufactured by Siemens Nuclear Power Corporation (SNP), formerly known as Advanced Nuclear Fuels (ANF), and designed to match the GE BP8DWB311-10GZ bundles neutronically and thermal-hydraulically. However, they differ from the GE bundles in the following ways: 1) the average bundle enrichment is lower, at 3.04 w/o U-235; 2) the fuel pins are smaller in diameter and their numbers are higher, at 72; and 3) a large square inner water channel is used rather than a large round water rod. The major mechanical design parameters are given in Table 9.1.1 and SNP's Generic Mechanical Design Report[30].

The bundles will be located at 05-22, 39-22, 05-24, and 39-24. These locations are expected to be nonlimiting with respect to MCPR, MAPLHGR, and MLHGR for the entire cycle during steady-state operation. The bundles will be monitored during the cycle to assure that they remain nonlimiting during steady-state operation. The use of the QFAs does not significantly affect the safety analysis described in Section 7.0[31]. VY specific calculations were also performed to show that the analyses in Section 7.0 bounded the ANF-IX QFAs. Therefore, the ANF-IX QFAs can be monitored as a GE bundle with conservative adjustments to the R-factor tables.

TABLE 9.1.1

Nominal ANF-IX Fuel Mechanical Design Parameters

Fuel Bundle*	
Bundle Types	ANF 9X9-IX
Vendor Designation	ANF-IX-3.04B-EGZ
Initial Enrichment, w/o U_{235}	3.04
Rod Array	9X9
Fuel Rods per Bundle	72
Outer Fuel Channel	
Material	Zr-2
Wall Thickness, inches	0.080

* Complete bundle, rod, and pellet descriptions are found in References 29 and 30.

10.0 STARTUP PROGRAM

Following refueling and prior to vessel reassembly, fuel assembly position and orientation will be verified and videotaped by underwater television.

The Vermont Yankee Startup Program will include process computer data checks, shutdown margin demonstration, in-sequence critical measurement, rod scram tests, power distribution comparisons, TIP reproducibility, and TIP symmetry checks. The content of the Startup Test Report will be similar to that sent to the Office of Inspection and Enforcement in the past[32].

REFERENCES

1. C. Chiu, Vermont Yankee Cycle 14 Summary Report, YAEC-1773, May 1991.

2. General Electric Standard Application for Reactor Fuel (GESTARII), NEDE-24011-P-A-10, GE Company Proprietary, February 1991, as amended.

3. A. S DiGiovine, J. P. Gorski, and M. A. Tremblay, SIMULATE-3 Validation and Verification, YAEC-1659-A, September 1988.

4. R. A. Woehlke, et al., MICBURN-3/CASMO-3/TABLES-3/SIMULATE-3 Benchmarking of Vermont Yankee Cycles 9 through 13, YAEC-1683-A, March 1989.

5. Report, B. Y. Hubbard, et al., End-of-Full-Power-Life Sensitivity Study for the Revised BWR Licensing Methodology, YAEC-1822, October 1991.

6. VYNPC Letter to USNRC, "Vermont Yankee LOCA Analysis Method: FROSSTEY Fuel Performance Code (FROSSTEY-2)," FVY 87-116, dated December 16, 1987.

7. Loss of Coolant Accident Analysis for Vermont Yankee Nuclear Power Station, NEDO-21697, May 1990, as amended.

8. Appendix A to Operating License DPR-28 Technical Specifications and Bases for Vermont Yankee Nuclear Power Station, Docket No. 50-271.

9. A. S. DiGiovine, et al., CASMO-3 Validation, YAEC-1363-A, April 1988.

10. A. A. F. Ansari, Methods for the Analysis of Boiling Water Reactors: Steady-State Core Flow Distribution Code (FIBWR), YAEC-1234, December 1980.

11. A. A. F. Ansari, R. R. Gay, and B. J. Gitnick, FIBWR: A Steady-State Core Flow Distribution Code for Boiling Water Reactors - Code Verification and Qualification Report, EPRI NP-1923, Project 1754-1 Final Report, July 1981.

12. USNRC Letter to J. B. Sinclair, SER, "Acceptance for Referencing in Licensing Actions for the Vermont Yankee Plant of Reports: YAEC-1232, YAEC-1238, YAEC-1299P, and YAEC-1234," NVY 82-157, September 15, 1982.

13. General Electric Company, GEXL-Plus Correlation Application to BWR 2-6 Reactors GE6 through GE9 Fuel, NEDE-31598P, GE Company Proprietary, July 1989.

14. A. A. F. Ansari and J. T. Cronin, Methods for the Analysis of Boiling Water Reactors: A Systems Transient Analysis Model (RETRAN), YAEC-1233, April 1981.

15. USNRC Letter to R. L. Smith, SER, "Amendment No. 70 to Facility License No. DPR-28," dated November 27, 1981.

16. V. Chandola, M. P. LeFrancois, and J. D. Robichaud, Application of One-Dimensional Kinetics to Boiling Water Reactor Transient Analysis Methods, YAEC-1693-A, Revision 1, November 1989.

17. Electric Power Research Institute, RETRAN - A Program for One-Dimensional Transient Thermal-Hydraulic Analysis of Complex Fluid Flow Systems, CCM-5, December 1978.

18. USNRC Letter to T. W. Schnatz, SER, "Acceptance for Referencing of Licensing Topical Reports: EPRI CCM-5 and EPRI NP-1850-CCM," September 4, 1984.

19. A. A. F. Ansari, K. J. Burns, and D. K. Beller, Methods for the Analysis of Boiling Water Reactors: Transient Critical Power Ratio Analysis (RETRAN-TCPYA01), YAEC-1299P, March 1982.

20. J. T. Cronin, Method for Generation of One-Dimensional Kinetics Data for RETRAN-02, YAEC-1694-A, June 1989.

21. C. J. Paone, et al., Rod Drop Accident Analysis for Large Boiling Water Reactors, NEDO-10527, March 1972.

22. R. C. Stirn, et al., Rod Drop Accident Analysis for Large Boiling Water Reactors Addendum No. 1, Multiple Enrichment Cores with Axial Gadolinium, NEDO-10527, Supplement 1, July 1972.

23. R. C. Stirn, et al., Rod Drop Accident Analysis for Large Boiling Water Reactor Addendum No. 2 Exposed Cores, NEDO-10527, Supplement 2, January 1973.

24. C. J. Paine, Banked Position Withdrawal Sequence, NEDO-21231, January 1977.

25. D. Radcliffe and R. E. Bates, "Reduced Notch Worth Procedure," SIL-316, November 1979.

26. M. A. Sironen, Vermont Yankee Cycle 14 Core Performance Analysis Report, YAEC-1706, October 1988.

27. General Electric Company, Loss-of-Coolant Accident Analysis for Vermont Yankee Nuclear Power Station, NEDO-21697, August 1977, as amended; NEDE-21697, Supplement 1, November 1987; and NEDE-21697, Supplement 2, May 1990.

28. Vermont Yankee Nuclear Power Station Final Safety Analysis Report, December 1991.

29. M. E. Garrett, K. D. Hartley, M. H. Smith, Vermont Yankee 9X9-IX Qualification Fuel Assembly Design Report, Mechanical, Thermal-Hydraulic, and Neutronic Design, ANF-90-034(P), Revision 0, SNP Company Proprietary, March 1990.

30. Siemens Nuclear Power Company, Generic Mechanical Designs for Advanced Nuclear Fuels 9X9-IX and 9X9-9X BWR Reload Fuel, ANF-89-014(P), SNP Company Proprietary, May 1989.

31. M. E. Garrett, K. D. Hartley, and M. H. Smith, Vermont Yankee Qualification Fuel Assembly Safety Analysis Report, ANF-90-048, May 1990.

32. L. A. Tremblay Letter to USNRC, "Cycle 15 Startup Test Report," BVY 91-10, January 23, 1991.

APPENDIX A

CALCULATED OPERATING LIMITS

The MCPR operating limits for the Reload Cycle are calculated by adding the calculated ΔCPR to the FCISL. This is done for each of the analyses in Section 7.0 at each of the exposure statepoints. For an exposure interval between statepoints, the highest MCPR limit at either end is assumed to apply to the whole interval.

Table A.1 provides the highest calculated MCPR limits for the Reload Cycle for each of the exposure intervals for the various scram speeds and for the various rod block lines. These MCPR operating limits are valid for operation of the Reload Cycle at full power up to 9845 MWd/St and for operation during coastdown beyond EOFPL.

Tables A.2 through A.5 provide the maximum calculated MAPLHGR limits for all the GE assembly types in the Reload Cycle.

TABLE A.1

Vermont Yankee Nuclear Power Station

Cycle 16 MCPR Operating Limits

Value of "N" in RBM Equation(1)	Average Control Rod Scram Time	Cycle Exposure Range	MCPR Operating Limit(2),(3)
42%	Equal to or better than L.C.O. 3.3.C.1.1	0 to 9845 MWd/St	1.32
	Equal to or better than L.C.O. 3.3.C.1.2	0 to 9845 MWd/St	1.32
41%	Equal to or better than L.C.O. 3.3.C.1.1	0 to 9845 MWd/St	1.28
	Equal to or better than L.C.O. 3.3.C.1.2	0 to 9845 MWd/St	1.28
≤ 40%	Equal to or better than L.C.O. 3.3.C.1.1	0 to 9845 MWd/St	1.23
	Equal to or better than L.C.O. 3.3.C.1.2	0 to 8241 MWd/St	1.23
		8241 to 9845 MWd/St	1.24

(1) The Rod Block Monitor (RBM) trip setpoints are determined by the equation shown in Table 3.2.5 of the Technical Specifications.

(2) The current analysis for the MCPR operating limits does not include the 7X7, 8X8, 8X8R or P8X8R fuel types. On this basis, if any of these fuel types are to be reinserted, they will be evaluated in accordance with the 10CFR50.59 to ensure that the above limits are bounding for these fuel types.

(3) MCPR operating limits are increased by 0.01 for the single loop operation.

TABLE A.2

MAPLHGR Versus Average Planar Exposure for BD324B

Plant: Vermont Yankee   Fuel Type: BD324B

Average Planar Exposure (MWd/St)	MAPLHGR Limits (kW/ft) Two-Loop Operation	Single-Loop Operation[*]
200.0	11.22	9.31
3,000.00	11.83	9.81
8,000.00	12.69	10.53
10,000.00	12.80	10.62
15,000.00	12.74	10.57
20,000.00	12.05	10.00
25,000.00	11.39	9.45
35,000.00	10.12	8.39
[illegible]00.00	8.46	7.02
50,000.00	5.99	4.97

[*] MAPLHGR limits for single-loop operation are obtained by multiplying the two-loop operation MAPLHGR limits by 0.83.

TABLE A.3

MAPLHGR Versus Average Planar Exposure for BD326B

Plant: Vermont Yankee

Fuel Type: BD326B

Average Planar Exposure (MWd/St)	MAPLHGR Limits (kW/ft) Two-Loop Operation	Single-Loop Operation*
200.0	11.26	9.34
3,000.00	11.72	9.72
8,000.00	12.76	10.59
10,000.00	12.90	10.70
15,000.00	12.82	10.64
20,000.00	12.12	10.05
25,000.00	11.44	9.49
35,000.00	10.15	8.42
45,000.00	8.63	7.16
50,000.00	6.17	5.12

* MAPLHGR limits for single-loop operation are obtained by multiplying the two-loop operation MAPLHGR limits by 0.83.

TABLE A.4

MAPLHGR Versus Average Planar Exposure for BP8DWB311-10GZ

Plant: Vermont Yankee

Fuel Type: BP8DWB311-10GZ

Average Planar Exposure (MWd/St)	MAPLHGR Limits (kW/ft) Two-Loop Operation	Single-Loop Operation*
200.0	11.00	9.13
6,000.00	11.92	9.89
7,000.00	12.11	10.05
8,000.00	12.34	10.24
10,000.00	12.83	10.64
12,500.00	13.00	10.79
20,000.00	12.24	10.15
25,000.00	11.55	9.58
45,000.00	8.76	7.27
50,740.00	5.[illegible]1	4.90

* MAPLHGR limits for single-loop operation are obtained by multiplying the two-loop operation MAPLHGR limits by 0.83.

TABLE A.5

MAPLHGR Versus Average Planar Exposure for BP8DWB311-11GZ

Plant: Vermont Yankee Fuel Type: BP8DWB311-11GZ

Average Planar Exposure	MAPLHGR Limits (kW/ft)	
(MWd/St)	Two-Loop Operation	Single-Loop Operation*
200.0	11.00	9.13
6,000.00	11.92	9.89
7,000.00	12.11	10.05
8,000.00	12.34	10.24
10,000.00	12.83	10.64
12,500.00	12.90	10.70
15,000.00	12.81	10.63
35,000.00	10.24	8.49
45,000.00	8.76	7.27
50,740.00	5.91	4.90

* MAPLHGR limits for single-loop operation are obtained by multiplying the two-loop operation MAPLHGR limits by 0.83.